Volume II

Appendices

to

EFFECT OF ENVIRONMENTAL VARIABLES AND SAMPLING MEDIA ON THE COLLECTION OF ATMOSPHERIC SULFATE AND NITRATE

(Contract No. ARB 5-1032)

Final Report

January 1978

Prepared by

B. R. Appel, Y. Tokiwa, S. M. Wall, E. L. Kothny
E. M. Hoffer, M. Haik and J. J. Wesolowski

Air and Industrial Hygiene Laboratory
Laboratory Services Branch
California Department of Health
2151 Berkeley Way
Berkeley, CA 94704

Table of Contents (Vol. II)

Appendix A

Calibration and Equivalency of High-Volume Air Samplers for Sulfate Sampling Study

The six hi-vol samplers were calibrated by the orifice plate technique. The "visifloats", normally employed on four of the units to monitor air flow, were replaced with a high quality rotameter for better precison. The rotameter was connected to the pressure tap on the air exhaust of the sampler motors when readings were desired. The remaining units had a continuous flow recorder which was calibrated in the usual manner. Before calibration, the voltage to each sampler motor was set to produce a flow rate of 44 cfm through the 18 hole resistance plate. At this voltage setting the resistance of a clean glass fiber filter (Gelman A) produced a flow of 40 cfm. At the start of each sampling run, the voltage of each sampler is set to the calibration value (monitored with a digital voltmeter) and the air flow noted. At the conclusion of the sampling period, the sampler voltages and air flows are recorded.

Following calibration, an experiment was conducted to establish the equivalency of total suspended particulate matter collected by six high-volume air samplers. The six samplers were operated on the roof of the State Department of Health building sampling the ambient atmosphere for each of six 24-hour periods. The samplers were arranged in an array as shown in Figure A-1. The positions of samplers #1, #2 and #3 were exchanged with those of samplers #4, #5 and #6, respectively, for the last two 24-hour sampling periods.

As the flow resistances of the preweighed glass fiber filters used in this experiment were higher than the filters used during flow calibration, the sampling flow rates were somewhat lower than expected. The flow resistance also appeared to be more variable among the preweighed filters producing a higher degree of flow rate variation between samplers than expected. To reduce the effects of relative humidity and handling on filter weights, all six filters were weighed just before sampling began and just after sampling was concluded for each day. All filter weighings were made on a Sartorius balance with an accuracy of 0.1 mg.

Table A-1 summarizes the data obtained for the six sampling days. The mean standard deviation in total suspended particulate matter (TSP) concentration for the sampling days was about 3.8%. The range in observed TSP concentration for a sampling period averaged about 9.4%.

Examination of the results by sampler suggest that unit number two gave consistently lower TSP values. This unit was probably the one which the sampling hut shielded most (see Figure A-1) even when its location was exchanged with sampler five for the last two runs.

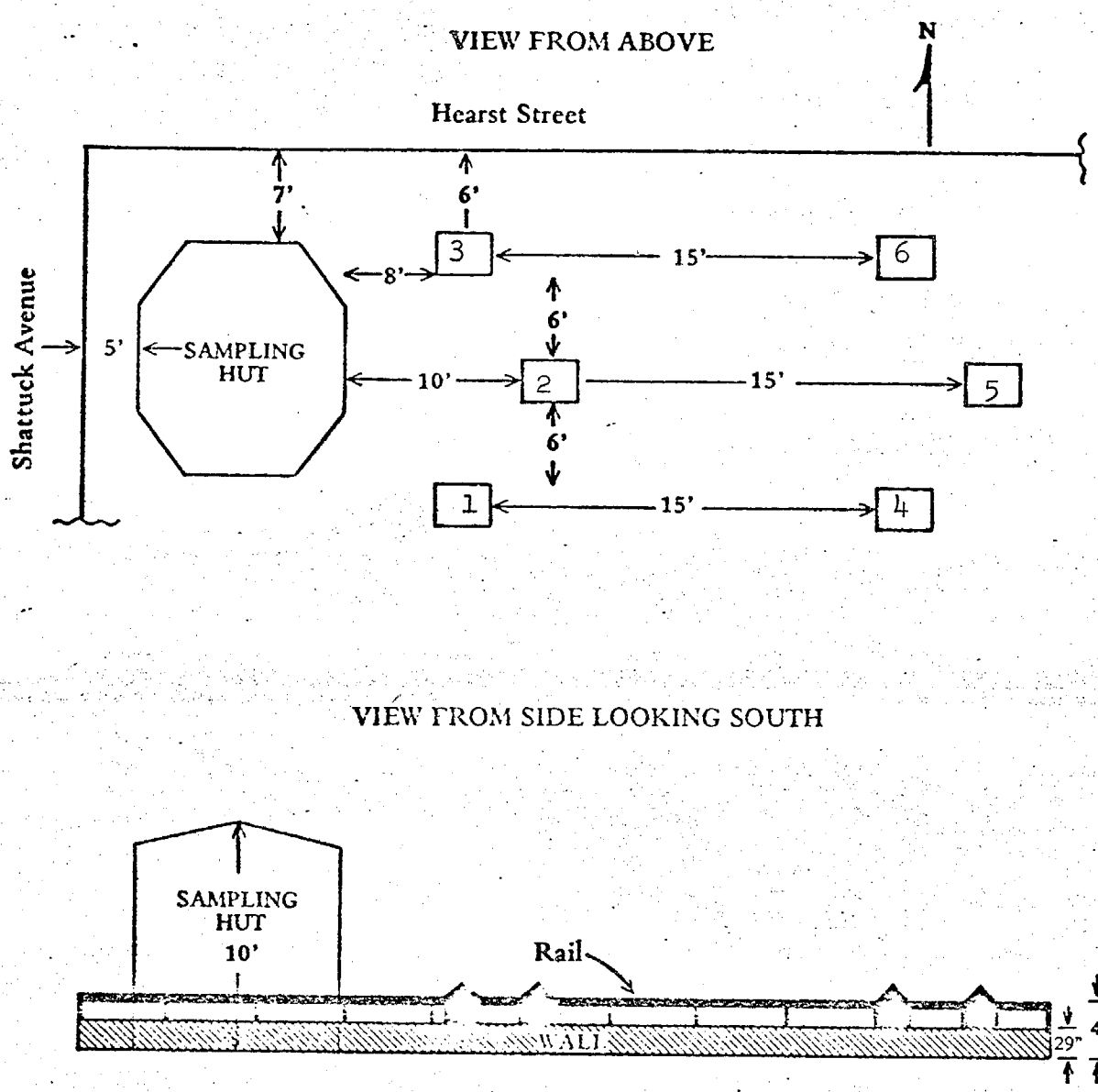

Figure A-1. Arrangement of High Volume Air Samplers on Roof of the State Health Department.

SOURCE: STATE OF CALIFORNIA
DEPARTMENT OF HEALTH
AIR AND INDUSTRIAL HYGIENE
LABORATORY, BERKELEY

Table A-1

Comparison of 24-Hour Average TSP Values for Six Hi-Vol Samplers

Run Simultaneously Using Gelman A Glass Fiber Filter

Run	Range in TSP, %[a]	Mean TSP ($\mu g/m^3$) $\pm$ 1 σ for 6 Samplers	Coefficient of Variation, %
1	8.9	56.4 $\pm$ 2.1	3.8
2	11	54.8 $\pm$ 2.6	4.7
3	13	36.8 $\pm$ 1.9	5.2
4	10	30.1 $\pm$ 1.2	3.8
5	7.3	39.8 $\pm$ 1.1	2.9
6	5.9	42.8 $\pm$ 1.1	2.5

[a] $\frac{\text{max value - min value}}{\text{max value}} \times 100$

Appendix B

Calibration of SO_2, O_3, NO_x and NH_3 Analyzers

1. Meloy Sulfur Analyzer

The Meloy flamephotometric detector relies on the photometric detection of the 394 nm-centered radiation emitted when sulfur-containing compounds are burned in a hydrogen rich air flame.

The unit was the same instrument used to monitor the ambient SO_2 background levels in the field sampling phase of the program. The calibration was rechecked after the field sampling by the AIHL calibration group. During the rechecking, however, the analyzer suddenly developed a malfunction. This was corrected by the ARB shop where a defective amplifier circuit board was replaced. A new calibration revealed the unit's response to SO_2 to be substantially the same as the previous calibration and the preliminary data obtained during the recheck indicated no change during the field study.

2. Bendix Ozone Analyzer

The Bendix Model 8002 Ozone Analyzer relies on the photometric detection of chemiluminescence that results from the gas phase reaction between ozone and ethylene. The instrument used was a U.S. Environmental Protection Agency unit on loan to the ARB. It was used at AIHL as the federal reference method to establish the equivalency of the ARB's DASIBI Ozone Monitor immediately prior to the present study.

3. TECO NO-NO_2-NO_x Analyzer

The TECO analyzer relies on the photometric detection of the chemiluminescent radiation produced by the reaction of NO with ozone. To measure NO_2, the NO_2 must first be reduced to NO. This is accomplished by passing the sample air through a heated (to 425°C) molybdenum alloy tube converter. According to the manufacturer, other nitrogen compounds including NH_3 are not affected. The NO_2 converted and the NO originally present in the sample is read out as NO_x. Direct readout for NO and NO_x are obtained by alternately passing the sample through the converter and bypassing it. A subtractor circuit subtracts the NO signal from the NO_x signal which is read out as NO_2.

The TECO analyzer used was a new unit acquired for this program. The unit was calibrated by the AIHL calibration group prior to installation.

As inferred earlier, the signal displayed is not continuous but rather cycles between the three pollutants. The time for a complete cycle is 1.5 minutes. For monitoring fast changing pollutant concentrations such as in filter isotherm studies such limitations are intolerable. To provide a continuous measure of the NO_2 concentrations in the isotherm studies with NO_2, the analyzer was operated in the NO_2 only mode (the analyzer displays only the subtractor signal). This is valid since the clean air contains NO_2 but no NO. To avoid the cycling between the three channels [NO, NO_2 and subtractor (NO_2) circuits], the subtractor signal was taken from the unit's front panel meter where the signal is continuous in this (NO_2) mode.

During the study, however, in contradiction to manufacturer's claims, the TECO registered 0.11 ppm in response to approximately 0.085 ppm NH_3. Although this was a familiar problem with earlier TECO units which used stainless steel converters operated at 900°C, the manufacturer was unable to satisfactorily explain the phenomena with this instrument. Experiences of the AIHL calibration group, however, indicate this to be an occasional problem with some converters. To obtain the true NO_2 concentration in the presence of ammonia, the following relationship was used:

$$\text{ppm } NO_2 = NO_{2(TECO)} - NH_{3(TECO)} - \text{baseline}$$

4. Lear Siegler NH_3 Analyzer

The Lear Siegler analyzer relies on spectrophotometric measurement of the absorption of ultraviolet light by ammonia gas molecules. Since the absorption of NH_3 in a cell path of six meter is small, slight fluctuations in the source intensity can mask changes in intensity due to absorption by NH_3. This deficiency is overcome in this instrument by sinusoidally varying the angular orientation of the photometer grating. This produces a monochromatic UV beam whose wavelength continually varies about the center band. Thus, the signal obtained is proportional to the curvature or slope of the intensity versus wavelength distribution and is independent of variations in the source lamp. Figure B-1 shows the arrangement and identifies the major components of the instrument.

The analyzer used was an ARB unit (Serial No. 1088) which was on loan to the Statewide Air Pollution Research Center at U.C. Riverside. Before use, the recommended maintenance tasks including cleaning and aligning the cell mirrors were performed. The instrument's electronics were adjusted using the instruments internal span cell (a quartz cell filled with NH_3 gas) as reference. In this process, however, it was found that the instrument's response was excessively low at the factory specified wavelength of 209 nm. The factory suggested replacement of the source lamp and realignment of the mirrors. This improved the response to the lowest value acceptable by the analyzer specifications. However, since operating at this level would require boosting the gain and thus amplifying the signal noise, 207 to 208 nm was used, increasing the gain to well within specifications.

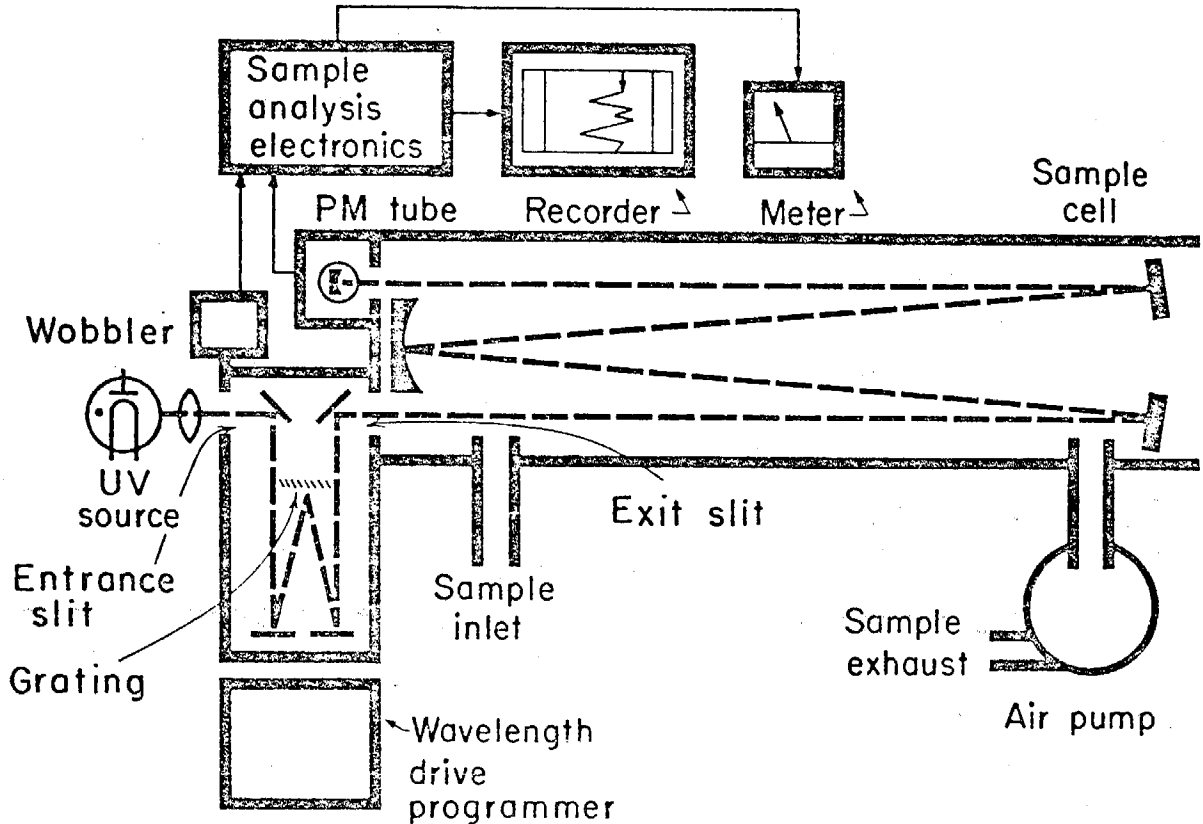

Figure B-1 *Second Derivative Spectrometer (Spectrometrics, Lear Siegler Incorporated)*

The instrument was then calibrated with air samples containing known concentrations of NH_3 from a calibrated permeation tube. The calibration data obtained for the analyzer are shown in Tables B-1 and B-2 and, for the analyzers in Figure B-2. The calibration also showed the instrument's internal span corresponded closely (0.25 ppm) to the 0.26 ppm specified by the factory.

The studies with mixed gases showed no response when subjected to NO_2 concentrations as high as 0.5 ppm. The instrument, however, responded negatively to SO_2; 0.1 ppm SO_2 registering as -0.25 ppm NH_3. The net NH_3 concentrations were calculated by subtracting the response due to the SO_2 (R_2) from the total response (R_1) as follows:

$$\text{ppm } NH_3 = R_1 - R_2$$

Table B-1

CALIBRATION

NH_3 PERMEATION TUBE

Manufacturer: Metronics
Length: 2 cm
Temp: 30°C
Rated Output: 320 ng/min/cm
Actual Output: 302 ng/min/cm

Date	Hour	Weight (gm)	Change (gm)	Loss (mg)
8/2	1015	2.5541	-	-
8/4	1018	2.5523	0.0018	1.8
8/6	1012	2.5506	0.0035	1.7
8/8	1020	2.5489	0.0052	1.7
8/10	1008	2.5470	0.0071	1.9
8/12	1000	2.5454	0.0087	1.6
8/18	1020	2.5402	0.0139	5.2

Table B-2

CALIBRATION

LEAR SIEGLER NH_3 ANALYZER

Air Flow			Response	
Set	L/min	ppm	Hi Range	Lo Range
3.5	1.9	0.46	0.45	-
4.0	2.4	0.36	0.34	-
6.0	4.2	0.21	0.22	-
10.0	8.2	0.11	0.12	-
12.0	10.2	0.085	0.09	0.085
16.0	14.5	0.060	0.05	0.055
18.0	16.8	0.052	0.04	0.050

Figure B-2

Calibration - Lear Siegler NH_3 Analyzer

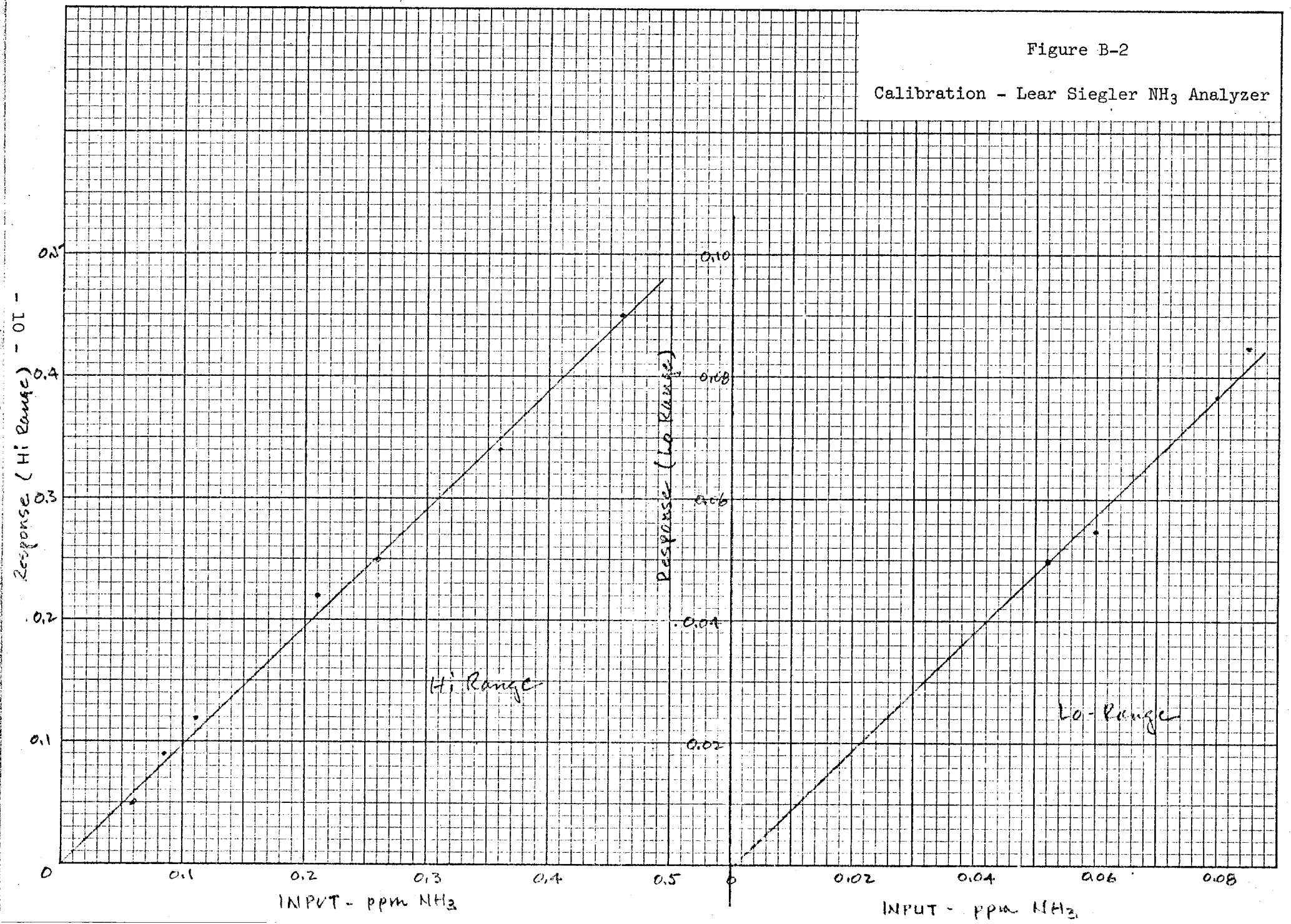

Appendix C

Nitric Acid Production

Anhydrous Liquid HNO_3 Preparation

The system employed to generate known concentrations of pure, anhydrous gaseous nitric acid is shown schematically in Figure C-1. The system was designed to permit vacuum distillation, collection and low temperature storage of the acid and subsequent preparation of dilute, gaseous nitric acid without exposure of the acid to ambient air. The distillation system is made of pyrex. Stopcocks were sealed with an inert, halocarbon grease (#25-55). The acid was prepared by distillation, at 0.2 torr, of a 1.3:1 mixture of concentrated sulfuric and nitric acids.[1] The temperature was maintained during distillation at 15°-20°C to avoid thermal decomposition of liquid nitric acid reported at > 30°C. To insure purity, the distillate was collected and stored in a cold trap at -80°C. The basic distillation protocol employed is as follows:

a. 100 ml of concentrated nitric acid (70%) was placed in the distillation flask and 130 ml of concentrated sulfuric acid (98%) was added to the pressure-equilizing delivery funnel. The HNO_3 was frozen at -80°C, and the system evacuated to < 0.2 torr.

b. The sulfuric acid was added slowly to the distillation flask allowing the exothermic reaction to thaw the nitric acid without raising the temperature of the mixture above 30°C.

c. After addition of sulfuric acid, a good distillation rate was achieved by heating with an infrared lamp to 15° to 20°C.

d. The middle fraction of distillate was collected by immersing the collection trap in a dry ice-acetone bath until 30-50 ml of frozen anhydrous acid were obtained.

e. The nitric acid was stored in the collection vessel at dry ice temperature under an atmosphere of dry nitrogen to prevent decomposition.

Preparation of 500-1000 ppm Nitric Acid in Dry Nitrogen

To provide a convenient means for injecting nitric acid vapor into the filter exposure system for prolonged periods, high concentrations (500-1000 ppm) of the anhydrous acid were prepared in a 30 ft^3 Tedlar bag. The bag was suspended in a large wooden enclosure to inhibit photodissociation and to allow external pressurization of the bag for nitric acid delivery into the exposure system air stream. To inhibit diffusion of water vapor through the Tedlar bag walls, the bag container was continuously flushed with quantities of dry air.

Bags containing known concentrations of nitric acid were generated by the following technique (see Figure C-1):

---

[1] L. Lloyd and P.A.H. Wyatt, J. Chem. Soc., 2248-2252 (1955).

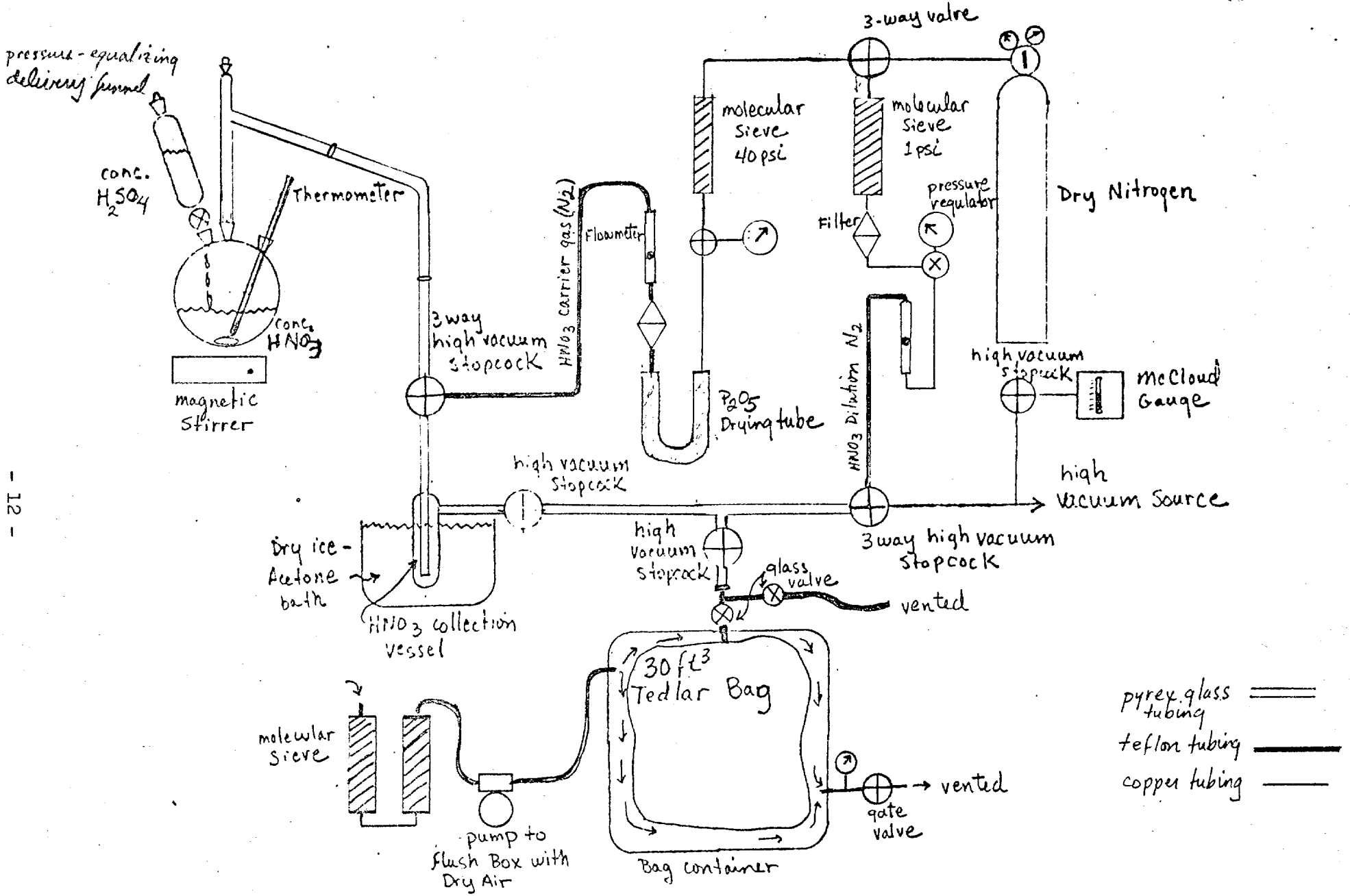

Figure C-1 Nitric Acid Generation and Dilution System

a. After evacuation and re-pressurization with dry nitrogen, the liquid nitric acid collection vessel was raised to 10°C in an ice water bath.

b. The bag was attached to the system and filled to half capacity with dry nitrogen.

c. A dry nitrogen carrier gas bubbling through the nitric acid vessel was used to transport the required quantity of anhydrous acid into the bag as calculated by the equations:

$$N_{HNO_3} = \frac{C_{Bag} \times FV_{Bag}}{10^6} \quad \frac{P_{ATM}}{R\ T_{Bag}}$$

where: N_{HNO_3} = moles of HNO_3 transported into Bag

C_{Bag} = desired HNO_3 concentration in Bag

FV_{Bag} = final volume of N_2 in Bag

P_{ATM} = pressure in Bag (1.0 ATM)

R = gas constant (0.08205)

T_{Bag} = temperature in Bag (298°K)

$$Vc.g. = \frac{N_{HNO_3} \times R \times T_{HNO_3}}{P_{HNO_3}}$$

where: Vc.g. = volume of N_2 carrier gas required to transport desired amount of HNO_3 into Bag

T_{HNO_3} = temperature at which HNO_3 evolved into carrier gas (283°K)

P_{HNO_3} = vapor pressure of HNO_3 at T_{HNO_3} (0.0348 ATM)

d. The bag was filled to a final volume of 30 $ft.^3$ with dry nitrogen which provided turbulent mixing of the bag contents.

e. The concentration in the bag was determined by collection of a bubbler sample and analysis by a nitrate specific ion electrode per the protocol outlined in Appendix E.

Dilute nitric acid (500-1200 ppm) was prepared reproducibly (within ± 10%) by this technique. Contamination from nitrogen oxides (NO, NO_2) proved to be less than 0.1% of the nitric acid level.

A stainless steel valve and rotameter were used to meter the nitric acid vapor (at 500-1200 ppm) into the filter exposure system where dilution to the desired concentration in the range 0.2 to 0.5 ppm was achieved.

Stability of Nitric Acid Bag Concentrations

Nitric acid concentrations were found to decrease significantly over a period of days after initial preparation. The mechanism for this effect appeared to be loss of nitric acid to the Tedlar bag walls rather than decomposition as no corresponding significant increase in nitrogen oxides was observed. Since the rate of nitric acid disappearance was reproducible, a decay curve was constructed to predict bag concentrations as a function of time after preparation (see Figure C-2). The decay curves were used to estimate collection times for the bubbler samples used to determine the bag concentration, such that the sample was within the analytical range of the nitrate specific ion electrode method. The bag contents were allowed to age for about 2 days.

Following this, although bag concentrations still decreased significantly, the decay rate was not fast enough (~ 0.5%/hr) to interfere with the production of stable nitric acid concentrations in the filter exposure system for up to 6-hour exposures.

Figure 2

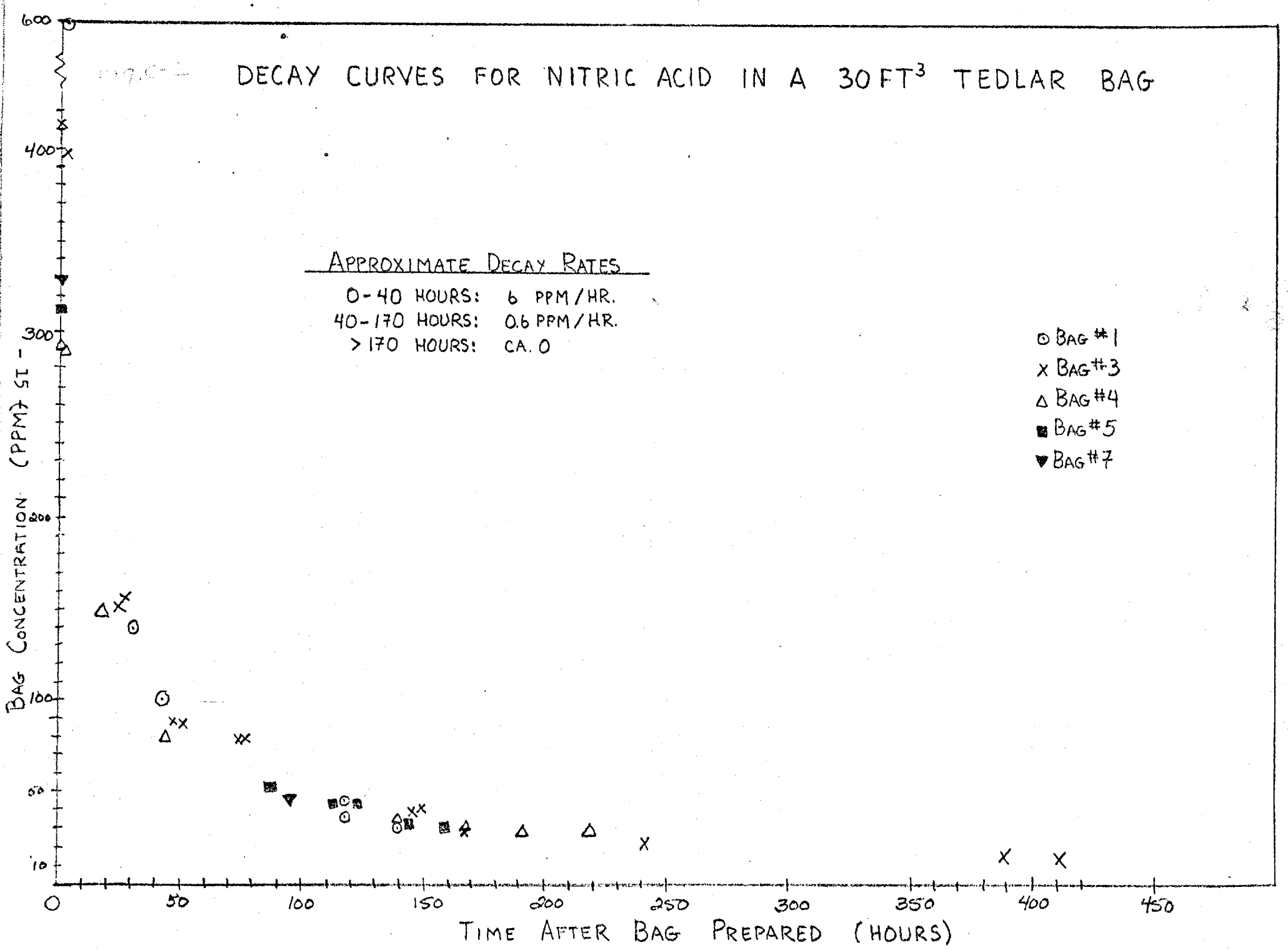
DECAY CURVES FOR NITRIC ACID IN A 30 FT³ TEDLAR BAG
APPROXIMATE DECAY RATES
0-40 HOURS: 6 PPM/HR.
40-170 HOURS: 0.6 PPM/HR.
>170 HOURS: CA. 0
BAG #1
BAG #3
BAG #4
BAG #5
BAG #7
BAG CONCENTRATION (PPM) SI -
600
400
300
200
100
50
10
0
50
100
150
200
250
300
350
400
450
TIME AFTER BAG PREPARED (HOURS)

Appendix D

Calibration of the Nitric Acid Monitors

The system used to calibrate the modified Mast microcoulomb meter and TECO chemiluminescence NO-NO_x analyzer for monitoring nitric acid is shown in Figure D-1. Concentrations of nitric acid in the range 10 to 20 ppm were prepared in a 30 $ft.^3$ Tedlar bag which served as a source of calibration gas. The calibration gas was metered into a dynamic dilution system where volumes of dry nitrogen were added to obtain various concentrations in the range 0.1 to 1.0 ppm. Uniformity of the resultant calibration gas concentration was assured by the use of two cyclone mixers ahead of the sampling ports for the nitric monitors. The calibration curves obtained for the instruments are included as Figures D-2 and D-3.

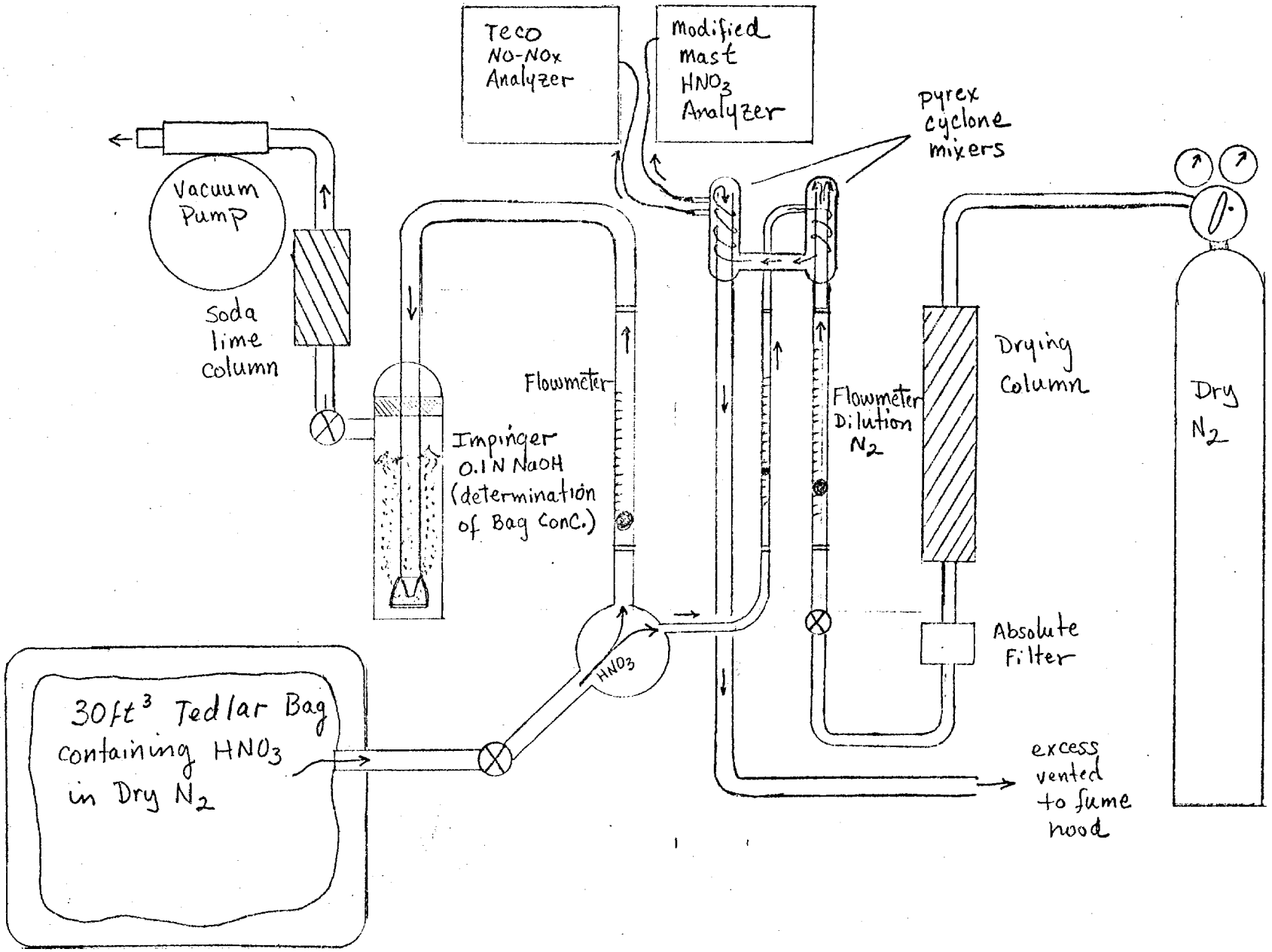

Figure D-1 HNO_3 Calibration System

Figure D-2

Calibration Curve for Mast HNO_3 Analyzer

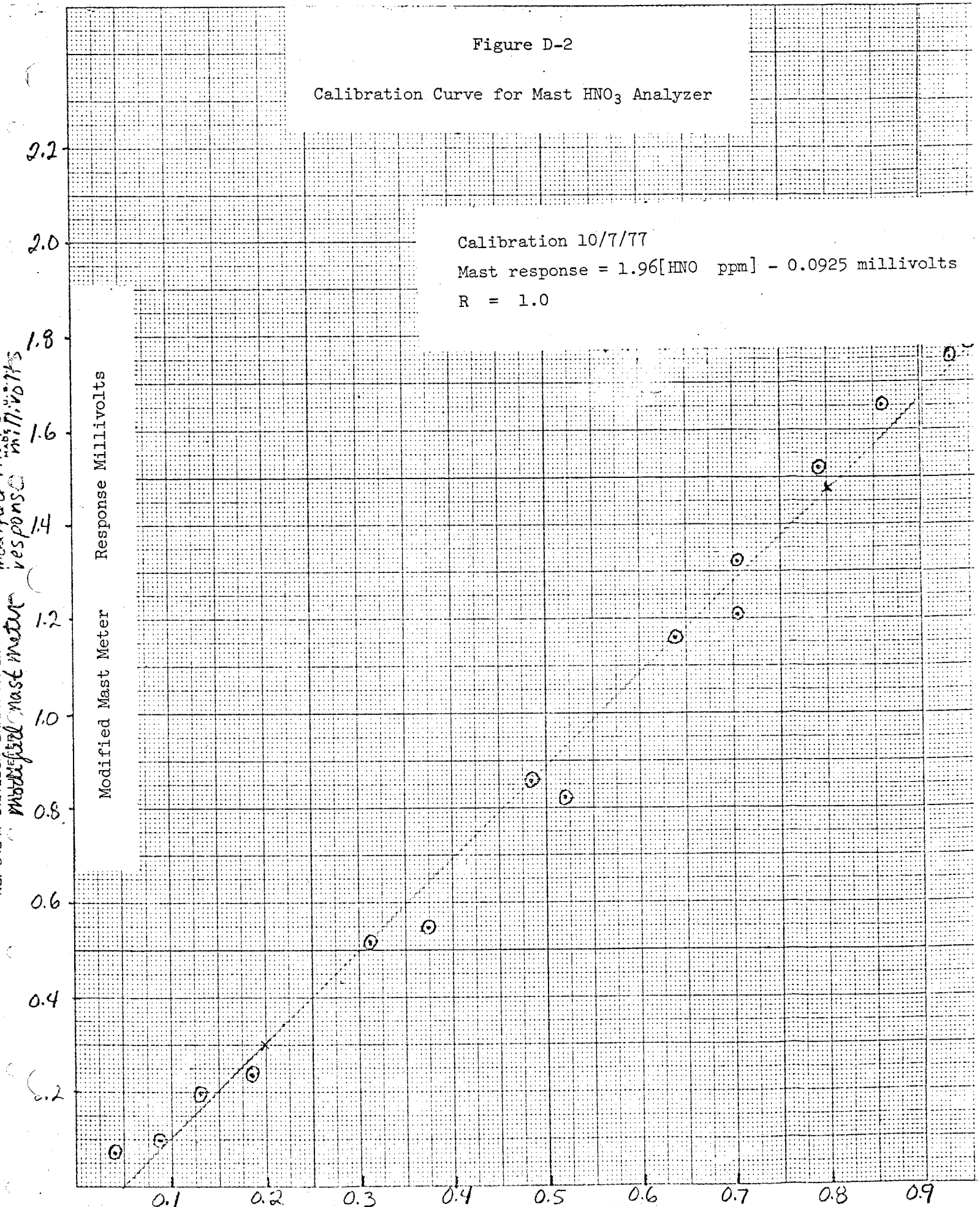

Figure D-3

Calibration Curve for TECO HNO_3 Analyzer

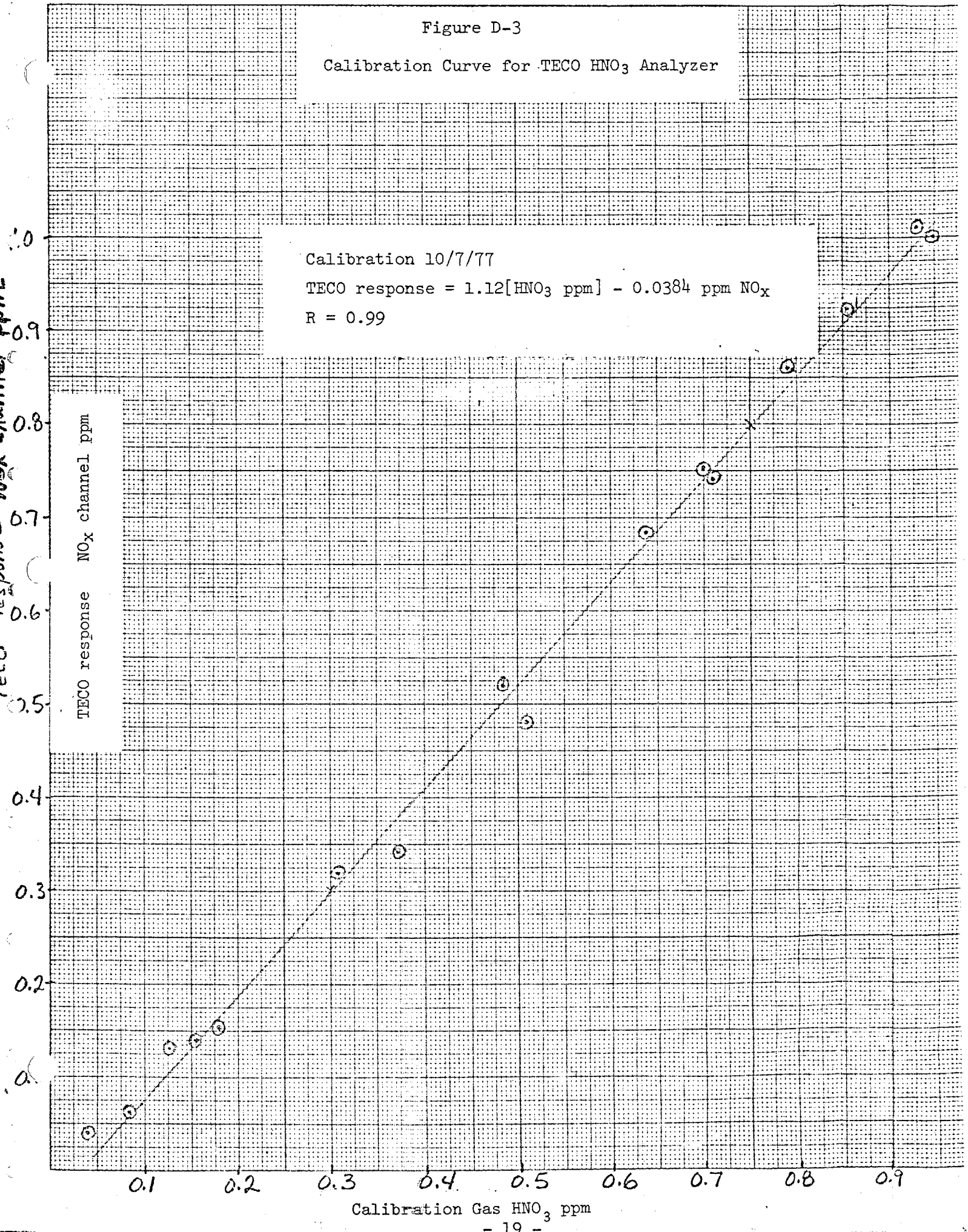

Appendix E

Protocol for the Determination of Nitric Acid by Specific Ion Electrode

by E. M. Hoffer

Scope

This is a special protocol to be used for nitric acid estimation when the nitric acid is sampled in 90 ml of 0.1N NaOH. (9 meq or 9 millimoles of NaOH). Since optimum performance for the specific ion electrode is in the pH range of 2-12, the 90 ml of 0.1N sodium hydroxide will have to be neutralized with 10 ml of 0.52M H_3PO_4 (5.2 millimoles of H_3PO_4) which will give approximately pH 7. One hundred ml of neutralized solution is obtained for analysis by the specific ion electrode.

Range and Sensitivity

Range is from 5×10^{-4}M to 10^{-2}M (about 30-600 µg/ml NO_3^-) for maximum reproducibility and accuracy.

Interferences

Ionic strength: A deviation of .01M-.025M ionic strength between the outer chamber filling solution and the sample reduces the accuracy of the measurement by 13-18% (12 measurements). The relationship between the difference in ionic strength of the outer filling solution and the accuracy of measurement appears non-linear.

Aging: Once stabilized, repeat measurements made after five hours may differ from the first set by 5% (mean of 10 determinations).

Temperature: According to the manufacturer, a 1°C change will produce a 2% error.

Precision and Accuracy

Coefficient of variation: This coefficient for a constant ionic strength set of samples with controlled temperature and timing was 0.9 $\pm$ 1.0% (8 determinations). Under conditions of a 10-25% variation from the optimal ionic strength, the coefficient increased to 3.0 $\pm$ 1.1% (12 determinations).

Accuracy: This parameter averaged 97 $\pm$ 1% over the range of 40 to 500 µg/ml. Samples with an ionic strength differing by 10-25% from the outer filling chamber solution, had an accuracy of 82-87%.

Apparatus

Orion Research Digital Analyzer Model 801A

Double junction reference electrode, Orion No. 90-02-00

Nitrate specific ion electrode, Orion No. 93-07

Sensing modules, Orion No. 93-07-01

There should be at least two nitrate sensing modules in good working order in case one stops functioning. The life of the nitrate module is six months.

100 ml screw top plastic containers

Box of disposable Pasteur pipets

Magnetic stirring bars (1" Teflon)

Magnetic stirrer. Should be of the type which remains cool during operation.

Thermometer

Timer

Reagents

Distilled or deionized water. All solutions should be made up with metal-free water.

Stock 1N NaOH

Take 50% solution of reagent NaOH, available in Stockroom, weigh out 80 g of the 50% NaOH solution, or 40 g NaOH pellets, and bring to 1 liter. This will give a 1.0N NaOH solution.

0.1N NaOH (for sampling HNO_3)

Prepared by diluting 100 ml of 1N NaOH to 1 liter. Transfer to a labeled plastic container.

0.520 M $H_3PO_4^-$

Weigh out 60 g of 85% H_3PO_4 (analytical grade, specific gravity 1.70 or 14.7 moles/liter) to fill to 1 liter. This will give $\frac{60 \times .85}{98}$ = 0.520 M H_3PO_4.

Nitrate Standard

0.1000 M $NaNO_3 \pm .0005$ Orion nitrate standard 92-07-06. Alternately weigh out 0.675 g $NaNO_3$ and fill to 500 ml.

Inner Filling Solution

Orion 90-00-02 colored filling solution.

Outer Filling Solution

Since ionic strength affects the operation of the electrode, the same ionic strength solution of the matrix in the sampling solution is used to fill the outer electrode. Take 90 ml of the same 0.1M NaOH solution used in sampling and add exactly 10 ml of 0.52M H_3PO_4. Mix, label and store in a clean bottle. This will be the outer filling solution. After filling leave electrodes in water and wait for at least half an hour to reach equilibrium. This practice seems to improve the correlation coefficient.

Procedure

Instrument Check-Out

Plug instrument in and leave on standby for at least 30 minutes or longer before check-out. It can remain in the standby position for immediate use over an extended time (months).

Connect shorting strap between rear panel sensing and REF jacks. Set the function switch to MV. The display should read 000.0 $\pm$ 000.1. If the reading deviates more, use a 3/32 inch screw driver to turn the zero adjustment screw (ZERO ADJ) until 000.0 is obtained. REL MV or pH setting is not checked since it is not used.

Electrode Check-Out

Double Junction Reference Electrode (Orion #90-02-00) - There is an inner and outer chamber to the reference electrode. Each chamber is filled with a different solution.

1. Inner Chamber

   Once per week the inner chamber liquid is replaced with Orion 90-00-02 colored filling solution. Unscrew cap and remove the spring. Insert the spout of a partially empty flip-spout bottle into the inner chamber, filling hole. With the bottle upright, the electrode upside down, and the inner chamber vent hole away from the user's body, squeeze the bottle. The filling solution will spurt out of the vent hole. Refill the inner chamber, place the spring on the electrode body, and screw the cap on finger-tight.

2. Outer Chamber

   Once each day before filling the outer chamber, drain the liquid by applying vacuum to the vent hole. Then use a disposable Pasteur pipet and fill the outer chamber. The level of the liquid in the outer chamber must be at least one inch above the level of the sample solution in the beaker.

Sampling and Nitrate Determination

Take 90 ml of 0.1N NaOH and place in the impinger, sample at 0.5-3 ℓ/min until 2-50 mg HNO_3 collected. Use a 90 ml calibration mark on the impinger to check if there was any volume loss. Bring to mark with water and then add 10 ml of 0.52 M H_3PO_4 to neutralize.* Transfer to a 100 ml screw top plastic container containing a one-inch magnetic stirring bar. Place sample on stirrer, insert electrodes, start vigorous stirring, set timer for 10 minutes, switch instrument from standby to MV. Check temperature on samples and standards to make sure there is not more than $\pm$ 1°C difference between them. After recording measurement, turn switch to standby. Remove electrodes, rinse off electrodes with distilled water, wipe with a tissue with a rapid downward stroke (which will remove water hanging at tip), but do not wipe the bottom of the nitrate sensing electrode. Place in the next test solution and continue in the same protocol. In making readings, it is best to proceed from dilute to increased concentration (important when calibrating).

Complete standards and samples within a total time period of one hour and 40 minutes since the error depends on the total time period. With 10 minutes per determination this permits running four standards and six unknowns. For determinations at a later time period, recalibrate with the same four standards before running other unknowns.

Calibration and Standards

Preparation of Nitrate Standards

In four 100 ml volumetric flasks, add the following:

Nitrate Standards	0.1 M Orion Nitrate	1 N NaOH	0.52 M H_3PO_4
5×10^{-4}M	0.500 ml	9 ml	10 ml
10^{-3}M	1.00 ml	9 ml	10 ml
5×10^{-3}M	5.00 ml	9 ml	10 ml
10^{-2}M	10.00 ml	9 ml	10 ml

using variable volume pipets, wherever possible.

Fill to mark with distilled water, mix and transfer to four labelled 100 ml screw top plastic containers with a 1" magnetic bar. Discard standards after a week. Keep tops on after use.

Calibrate the instrument and calculate the slope. The slope should be constant to $\pm$ 1 and the correlation coefficient should be better than .996. Check out all the nitrate sensing modules in the set to determine if they are in working order. Always keep two modules on hand.

*Ionic strength can be monitored with a refractometer.

Calculation

Using a log/linear paper, plot the nitrate concentration in moles/liter or µg/ml on the logarithmic scale (x) and the millivolts on the linear scale (y).

While making the determinations, read the corresponding concentration in moles/ℓ. From this plot, gross errors in linearity can be immediately detected. If the slope is off, and the standards are right, then the nitra e sensing electrode is off. In this case, change to another sensing electrode.

Calculate the regression with the program for a semi-log regression curve. The available program will give intercept, slope and coefficient of correlation. Then calculate the unknown concentrations (x) from the millivolt readings (y).

Appendix F

Determination of Reactive Silicate*

Reactive silicates are those forms of silicate which react with molybdic acid to give the silicomolybdate complex. Generally, only monomeric or dimeric silicates react whereas higher polymers do not. Silicates easily depolymerize at higher pH. Since glass fiber filters are believed to be the dominant source of silicate in the current program, and these are made out of relatively alkaline compositions, it is assumed that most of the soluble silicate in the extracts is reactive.

The critical step in the method is the formation of silicomolybdate which involves a rapid adjustment of the acidity of the sample in the presence of molybdic acid. This is accomplished by adding the sample extract to a mixture of molybdic acid and hydrochloric acid (and not vice versa). After 10 to 15 minutes, the reaction is assumed to be essentially complete. Once the silicomolybdate complex has formed, it can be either measured directly or changed to molybdenum blue and measured at ca. 800 nm. The silicomolybdate complex absorbs at 320/330 nm, but molybdic acid also absorbs strongly in this region. This overlap makes the determination imprecise especially if a tungsten filament light source is used. Therefore, conversion to the blue compound is preferable.

Sensitivity for the blue compound is about 2 to 3 times higher than for the species read in the UV.

The reducing substance recommended in the paper is p-methylaminophenol. Since this compound was not available to us, we tried several other reducing compounds generally used for molybdate blue methods. In our trials, 4 compounds tested gave essentially the same results:

	Absorbance at 810 nm with 1 ppm SiO_2
p-aminophenol (most similar to the substance recommended)	0.58
ascorbic acid	0.54
1, 2, 4 aminonapthol sulfonic acid	0.54
o-phenylenediamine	0.56
hydrazine	0.43

*The method used is based on information detailed in the book "Fisheries Research Board of Canada, Bulletin No. 125, 2nd Ed. 1965: A Manual of Sea Water Analysis, by JDH Strickland and TR Parsons." Modifications, discussed here were made in the reducing agent and volumes of reagents and samples.

[1]VW Truesdale and CJ Smith: The spectrophotometric Characteristics of Aqueous Solutions of α + β Molybdosilicic Acids. Analyst 100, 797-805, 1975.

In all cases except with hydrazine, sodium bisulfite was added as a preservative. Hydrazine was eliminated because of the slowness of the reaction. In most methods using hydrazine, this subtance is heated to hasten reaction. All the organic substances except ascorbic acid were eliminated because of their yellow color, either before or after the reaction. A stock solution containing ascorbic acid and bisulfite in equal amounts has been found to remain stable for about one month. This same reducing substance was also suggested by Murphy and Riley[2] for the analysis of phosphate for reduction of phosphomolybdic acid to the corresponding Mo-blue. Other modifications to the original method involved proportionate reductions of volumes to scale the method to the samples analyzed.

Method for the Determination of Reactive Silicate in Small Samples of Aqueous Extracts from Atmospheric Particulate

Reagent A: 80 ml of 2% ammonium molybdate solution

9 ml of 6 M hydrochloric acid

Make up to 100 ml. The solution is usable indefinitely unless a precipitate is seen.

Reagent B: In a 100 ml stoppered cylinder mix:

55 ml of 5 N H_2SO_4 (70 ml conc. H_2SO_4 to 500 ml with water)

15 ml of saturated oxalic acid solution (approx. 10%)

25 ml of 1% ascorbic acid containing 1% of sodium bisulfite

Make up to 100 ml. Discard after 24 hours.

Procedure: In 10 ml Erlenmeyer flasks, place 1 ml of reagent A and add 5 ml of sample solution. Let react for 15 $\pm$ 5 min.

Add 4 ml of reagent B and let react for one hour $\pm$ 15 min.

Measure at 810 nm against a blank made with distilled water.

Compare with a calibration curve made with standards containing a maximum of 2 ppm SiO_2.

Standard: A 100 ppm SiO_2 solution is made by diluting 4.67 ml of a 1000 µg/ml Si standard (commercially available).

[2]Murphy and JP Riley: A modified single solution method for the determination of phosphate in natural waters. Anal. Chim. Acta, 27 (1962), 31-36.

Range: With a 20 mm (or 25 mm) cell, the range is 0.2 to 2 µg/ml SiO_2.

With a 10 mm cell, the range is 0.5 to 4 µg/ml SiO_2.

With a 1 mm cell (10 mm cell + 9 mm spacer), the range can be extended to 40 µg/ml SiO_2.

Precision: The precision is better than 5% at all levels, when standards are run concurrently with the samples.

Working Curve: Figure F-1 shows a typical working curve used for silicate. Where only one point is visible, the two determinations were indistinguishable.

FIGURE F-1

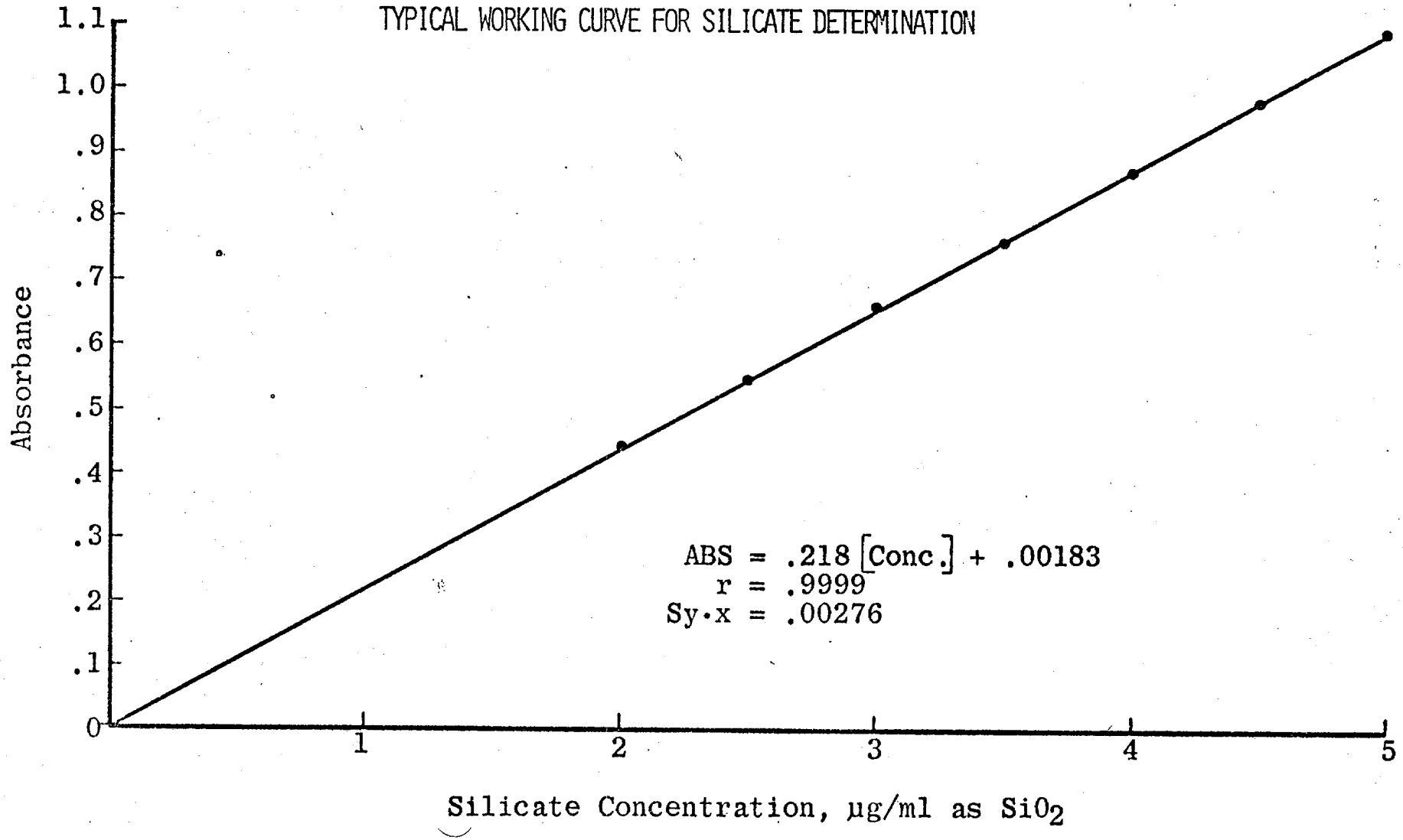
TYPICAL WORKING CURVE FOR SILICATE DETERMINATION
Absorbance
1.1
1.0
.9
.8
.7
.6
.5
.4
.3
.2
.1
0
1
2
3
4
5
ABS = .218 [Conc.] + .00183
r = .9999
Sy·x = .00276
Silicate Concentration, µg/ml as SiO_2

Appendix G

Determination of Phosphate

Introduction

The chemistry of molybdenum blue formation was exhaustively studied in the past three decades and as a result many methods for phosphate, silicate, arsenate, germanium and other metals were described. Generally, these methods are not specific and are cumbersome. Higher specificity can be obtained, however, by employing low pH, organic reducing substances and complexing agents. The method for phosphate was improved by selecting appropriate conditions which enable the use of a single solution (1, 2) for the analysis. The procedure used here is a minor modification of the method in references 1 and 2. Changes involved a proportional reduction of the amounts of reagent which was necessary to handle the small samples available.

Interferences

In this method, the only interferent of any significance is arsenate, which is 0.4 times as sensitive as phosphate. This element is only rarely occurring in concentrations affecting the phosphate results (the natural ratio is < 1:20). The color is measured either at 710 or 882 nm. About 20% higher sensitivity can be achieved when measuring at 882 nm. However, this wavelength is near the cut-off limit of most instruments and causes large instabilities. The second peak at 710 nm was chosen for use with our instrumentation. The concentration of the complexing metal, antimony, must be below 8 µg/ml to avoid clouding. The blue complex contains phosphorus and antimony in a ratio of about unity.

Reagents

Mix 32 ml of 5 N H_2SO_4 (made by diluting 70 ml conc. acid to 500 ml)

20 ml of 2% molybdate

35 ml of 1% ascorbic acid solution containing 1% Na bisulfite

3 ml of 1 mg/ml solution of Sb (0.274 g of K Sb tartrate to 100 ml)

Fill the mixture to 100 ml with distilled water and discard after 24 hours.

Procedure

To three ml of sample solution add one ml of the reagent mixture. When using a 25 mm cell, these volumes must be doubled. Measure at 710 nm after 10 to 15 min.

Range

A range of 0.3 to 4 ppm can be covered with a 25 mm cell. With shorter pathlengths, e.g., 10 mm, up to 80 ppm can be measured directly. Higher concentrations need aliquoting and dilution of samples.

Standards

The 1000 ppm $PO_4^{\equiv}$ standard is made by dissolving 0.286 g KH_2PO_4 in 200 ml of distilled water. Dilute 1 ml to 100 ml with water for the working standard of 10 ppm. With a repetitive pipet make dilutions covering the desired range.

Working Curve

Figure G-1 illustrates the working curve used as prepared from standards run before and after the samples. Where only a single point is shown the two determinations are indistinguishable.

1. J. Murphy and J. P. Riley: A modified single solution method for the determination of phosphate in natural waters. Anal. Chim. Acta 27, 31-36, 1962.

2. S. J. Eisenriech, R. T. Bannerman, D. E. Armstrong: A simplified phosphorus analysis technique. Environmental Letters 9(1), 43-53, 1975.

Figure G-1

CALIBRATION CURVES FOR PHOSPHATE DETERMINATION

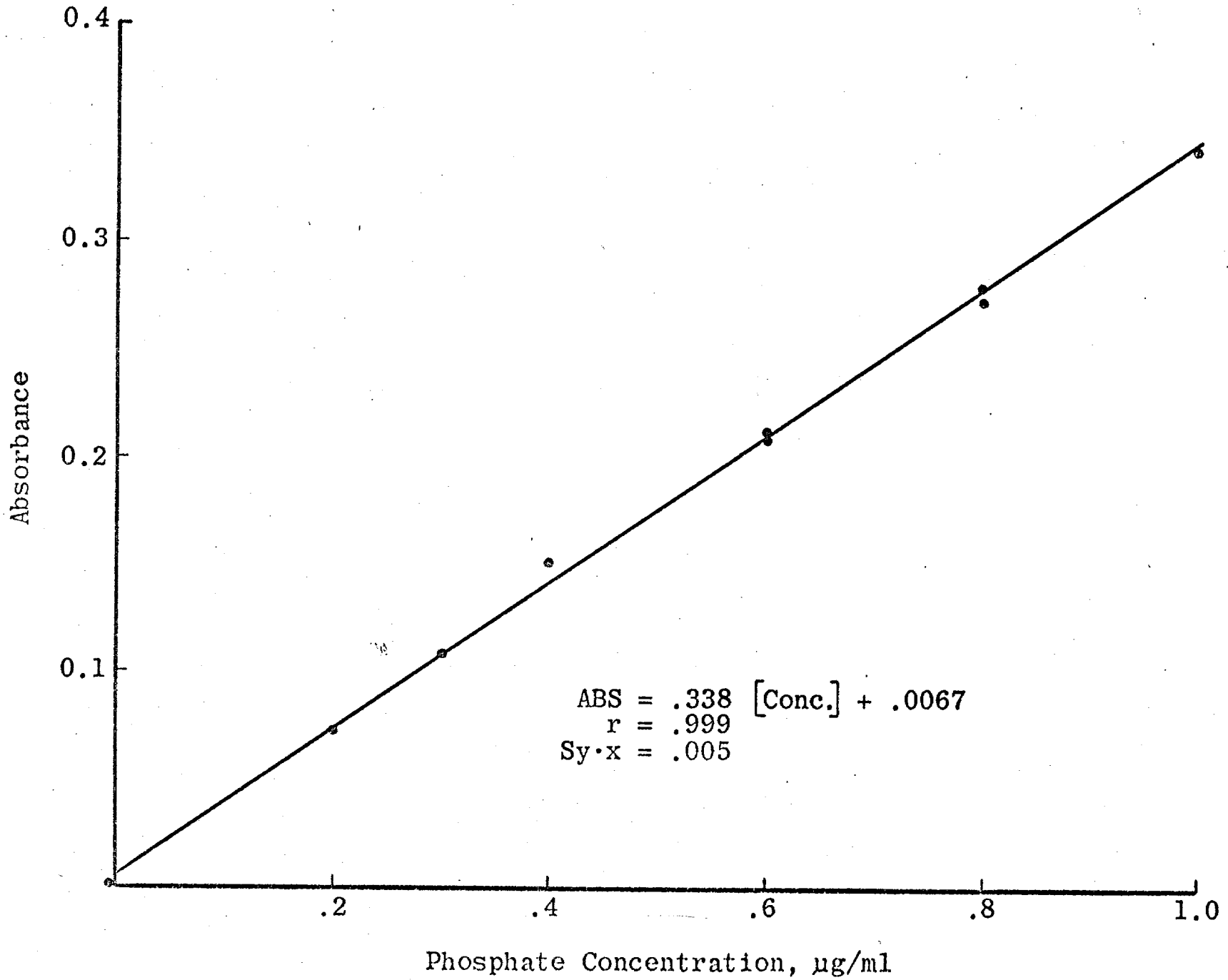

Appendix H

Determination of Sulfite

Filter discs were placed into 100 ml plastic screw cap vials containing 10 ml of 0.04 M tetrachloromercurate. The containers were capped and immersed into a minimal depth of water inside a sonicator bath for one minute.

After removal from the bath, the vials were uncovered and the following reagents were added.*

1 ml of 0.6% sulfamic acid. After 10 min. stabilization,

2 ml of a 1:200 dilution of 40% formaldehyde,

5 ml of pararosaniline solution (20 ml purified 0.2% pararosaniline diluted with 200 ml 3 M H_3PO_4 and 30 ml distilled water) and

2 ml of distilled water. The total volume was 20 ml.

After 20 min. reaction time, each filter sample was filtered by gravity through a 7 cm No. 40 Whatman filter into a dry test tube 16 x 200. The absorbance was measured at 580 nm in a 5 cm cell against water. A calibration line was measured concurrently. This was prepared by measuring aliquots of a precalibrated 10 µg/ml SO_2 solution in tetrachloromercurate. Figure H-1 shows a typical working curve.

*Adapted with the modifications indicated for maximum sensitivity from Method 42401-01-69T, Intersociety Committee: Methods of Air Sampling and Analysis, American Public Health Association, 1972, Washington, D.C., pp 447-455.

SULFITE CALIBRATION CURVE

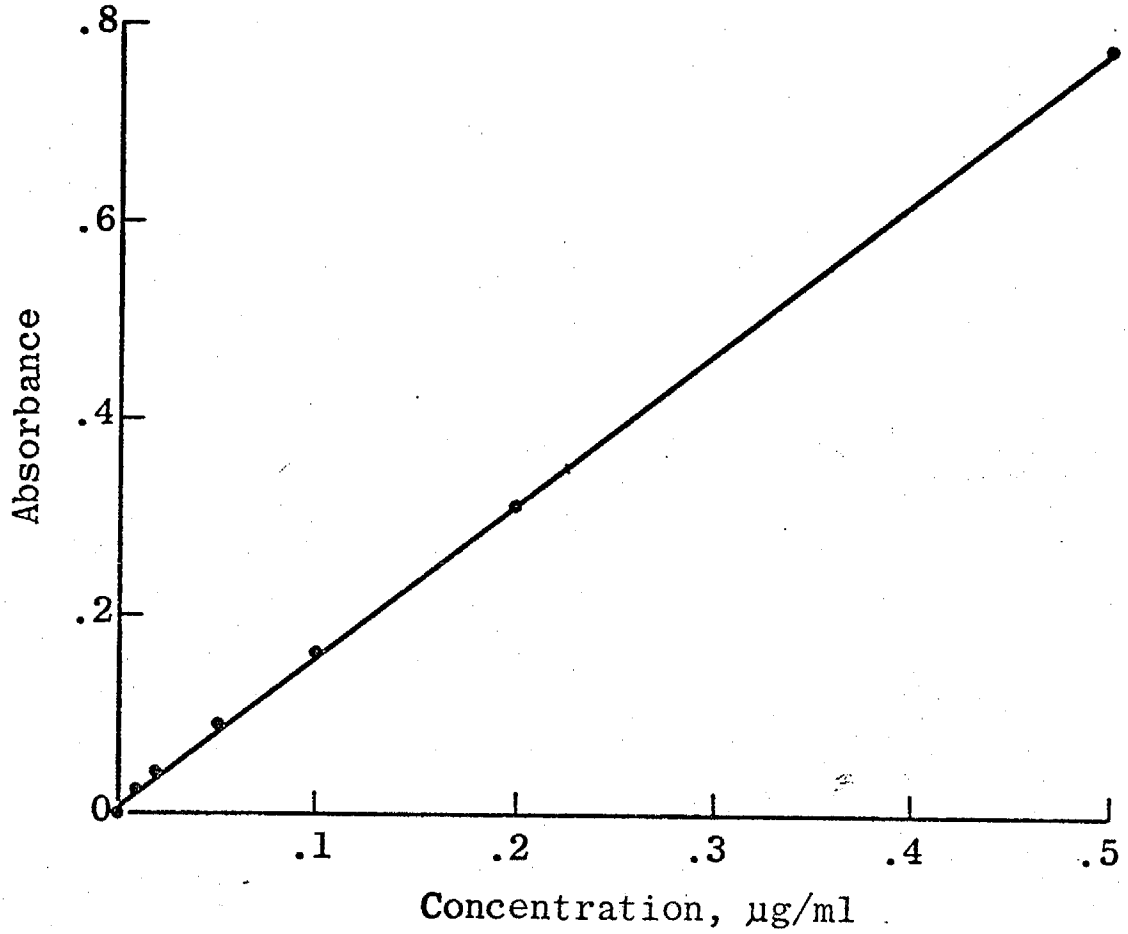

ABS = .007 + 1.53 [Conc.]
Sy·x = .0021

Figure H-1

MEASUREMENTS OF THE FILTRATION EFFICIENCIES OF SELECTED FILTER MEDIA

Prepared by:

Walter John and Georg P. Reischl

With partial support from:

Air Resources Board Grant 5-1032

January 1977

Air and Industrial Hygiene Laboratory
Laboratory Services Branch
California Department of Health
2151 Berkeley Way
Berkeley, California 94704
(415) 843-7900, ext. 595

MEASUREMENTS OF THE FILTRATION EFFICIENCIES OF SELECTED FILTER MEDIA

ABSTRACT

The filtration efficiencies of selected filter media have been measured with pressurized room air and a condensation nuclei counter. The room dust particles were predominately less than one micrometer in diameter. Lower limits ranging from 99.0 to 99.9% were established for the efficiencies of Gelman Spectrograde glass fiber, Fluoropore (1 μm pore), Gelman GA-1 cellulose acetate, MSA glass fiber, Gelman A glass fiber and EPA glass fiber filters. Nuclepore (0.8 μm pore) and Whatman 41 filters were found to have much lower efficiencies. The effect of pressure on filtration efficiency is discussed. At high flowrates the pressure drop across Fluoropore is found to increase with time even with clean air.

INTRODUCTION

The filtration efficiencies of several commonly-used filter media have been measured using room dust. The object was to determine the initial efficiencies for submicrometer particles such as found in ambient air. These measurements were undertaken in support of an AIHL project, Effect of Environmental Variables and Sampling Media on the Collection of Atmospheric Sulfate, supported by the Air Resources Board.

Although the filtration efficiencies of some of these filters have been measured before,[1] it seemed advisable to remeasure them. In addition, a new Teflon membrane filter medium, Fluoropore, became available. The Teflon membrane appears to be promising for sulfate sampling because of a low tendency to catalyze the conversion of sulfur dioxide to sulfate.

The use of a condensation nuclei counter (CNC) to detect the dust particles afforded high sensitivity for submicrometer particles but required a special arrangement for the measurements. The CNC operates properly only in a very narrow range around atmospheric pressure. Because of the high pressure drop across the filters, it was necessary to compress the dust-laden air, pass it through the filter and measure the particle penetration on the downstream side at atmospheric pressure. Ordinarily, in sampling ambient air, the air is pumped from atmospheric pressure to a partial vacuum on the other side of the filter. A critical discussion of the effect of pressure on filtration efficiency is presented below and it is concluded that the presently-measured filtration efficiencies also apply to the sampling of ambient air within the accuracy of the measurements.

EXPERIMENTAL PROCEDURES

The room in which the measurements were conducted was not air conditioned and a window was open to the outside. A block diagram of the experimental arrangement is shown in Figure 1. An oil-less compressor with the inlet filters removed supplied air to a storage tank. The two valves shown in Figure 1 were adjusted to provide the desired flow rate through the filter and to maintain a total flow rate of approximately 85 ℓpm (3 CFM). At this flow rate the compressor operates continuously, thus maintaining the dust input from the room.

The 47 mm filters were placed in an inline aluminum filter holder, Gelman Model 1235*, which has an O-ring at the periphery providing a positive seal to the filter and to the outside. The filters are supported by a photo-etched stainless steel screen. A 35 mm diameter area of the screen is perforated by 130 μm diameter holes spaced 256 μm apart. The total area of the holes is 21% of the 9.62 cm^2 defined by the 35 mm diameter circle. There is therefore some uncertainty as to what area to use to calculate face velocities. Following the usual practice we have used 9.62 cm^2 as the effective area, which gives a lower limit for the calculated face velocity.

---

*The mention of commercial products, their source or their use in connection with material reported herein is not to be construed as either an actual or implied endorsement of such products.

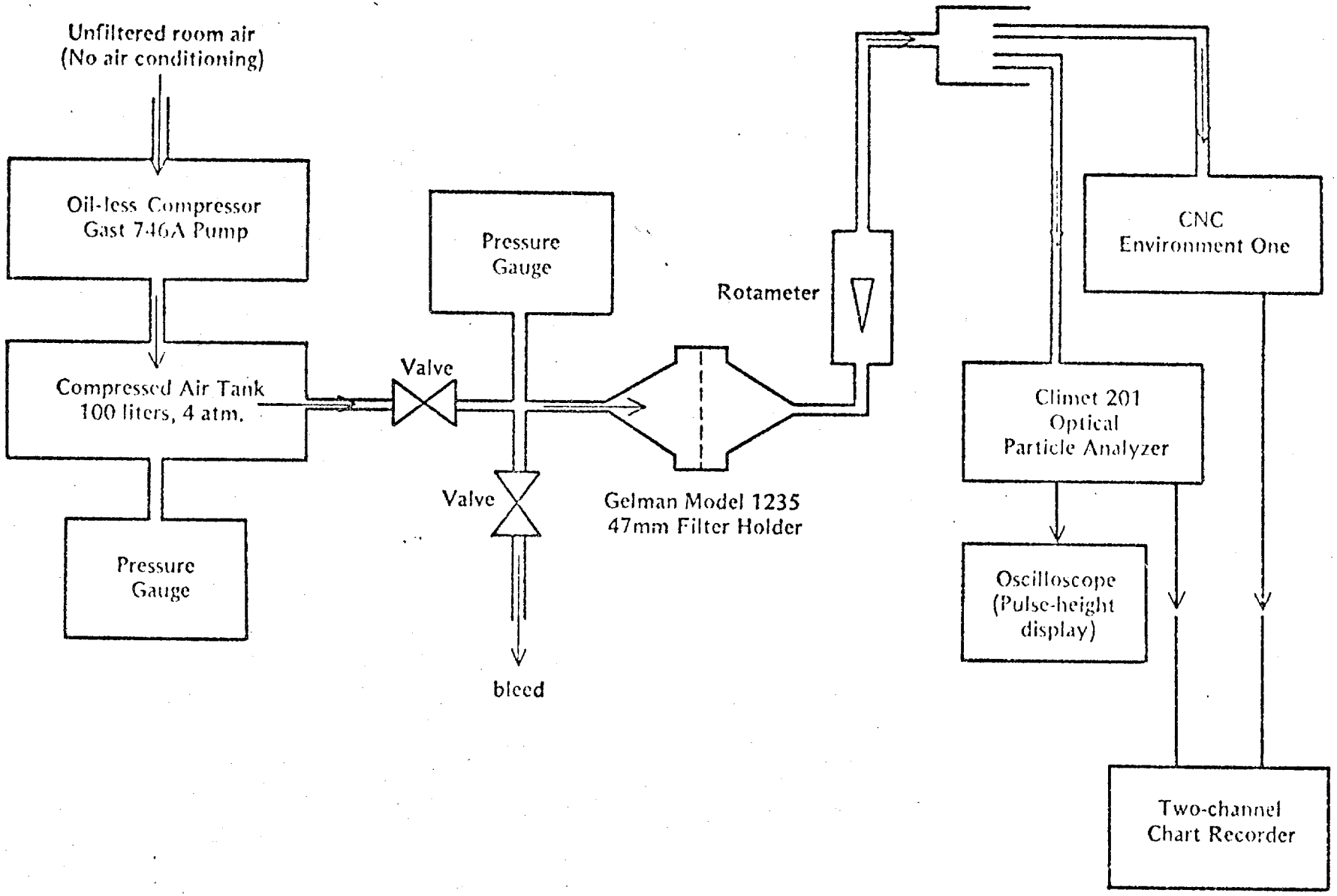

Figure 1 - Experimental arrangement for filter efficiency measurement

Each filter was examined for pinholes; only filters free of defects were used. The air pressure was measured on the upstream side of the filter. This pressure reading provided an additional check on the soundness of the filter as well as on the seal of the filter holder. The pressure drop across the filter itself was determined by subtracting the pressure reading at the same flow rate with the filter removed.

A rotameter downstream of the filter and hence at atmospheric pressure was used to determine the flow rate. Most of the measurements were made at 28.3 ℓpm (1 CFM) and at 84.9 ℓpm (3 CFM). At 28.3 ℓpm the face velocity (using 9.62 cm^2 effective area) is 49 cm/s, a typical value obtaining for ambient air sampling. The 84.9 ℓpm was considered to be near the maximum flow rate of interest; indeed, it appears that this flow rate is excessive for Fluoropore as discussed below. The Fluoropore filtration efficiency was measured at a number of flow rates extending down to 3 ℓpm.

A condensation nuclei counter (Environment One) was used to count particles in the air downstream of the filter holder. The CNC is specified by the manufacturer to count particles down to 0.0025 μm diameter. The counter calibration by the manufacturer was based on a Pollak counter. Typically, with no filter in the holder, the CNC count was 22,000 particles/ml. A Climet optical particle analyzer was also used to obtain information on the size distribution of particles greater than 0.3 μm diameter. Based on both counters, typically 99.9% of the particles in the room air were less than 1 μm in diameter.

Filtration efficiency e is defined by

$$e = 1 - \frac{N_2}{N_1}$$

where N_1 is the number of particles incident on the filter and N_2 is the number penetrating the filter. N_1 and N_2 were determined in the present measurements by taking the CNC count (particles/ml) without and with the filter in place. Careful consideration shows that no corrections for volume changes are necessary, the only assumption being that the mass of particles per mass of air remains constant. Since the particles are sub-micrometer in size they follow the streamlines, making this a good assumption.

The background was determined by sampling air filtered by a pleated membrane. The background was normally about 100 particles/ml but with tuning of the CNC electronics could be as low as 35 particles/ml, indicating that most of the background count originated in the instrument and not from particles penetrating the pleated membrane. For filters giving a CNC count equal to the background, an upper limit to the particle penetration was assigned to be 35 particles/ml. Prior to the tests of the Gelman GA-1 and the MSA filters, repairs to the CNC were made, resulting in an increased and less reproducible background (140 to 180 particles/ml). Therefore for these runs we have assigned a conservative upper limit to penetration equal to the total observed background count.

EXPERIMENTAL RESULTS

A. Filter Efficiencies

The measured filtration efficiencies are listed in Table I. For Gelman Spectrograde glass fiber, Fluoropore, Gelman GA-1, Gelman A and EPA glass fiber and MSA filters, no particle penetration was detected and the lower limits to the filtration efficiencies range from 99.0 to 99.9%. By contrast, fairly high penetrations of the Nuclepore and Whatman 41 filters were observed. These results are in general agreement with previous work.[1]

We note that the new medium, Fluoropore, had a > 99.9% efficiency from 3 ℓpm to 84.9 ℓpm. These findings agree with newly published work by Liu and Lee.[2]

B. Pressure Drop Across Fluoropore Filters

In the course of this work we noticed that the pressure drop across Fluoropore filters increased with time at high flow rates. In Figure 2, the pressure drop across the filter is plotted for the first 10 minutes for three different flow rates using clean air. No change with time is seen at 28.3 ℓpm. At 56.6 ℓpm a small increase occurs during the first two minutes. At 84.9 ℓpm the pressure drop is still increasing after 10 minutes. In Figure 3 the pressure drop is shown for several hours for two different filters. The pressure drop approximately doubles in 3 hours and is still rising.

The observed increase in pressure drop can probably be attributed to mechanical creep of the Teflon filter material. This would tend to

Table 1

MEASURED FILTRATION EFFICIENCIES

Filter Type	Flowrate ℓpm	Number of Filters Tested	Filtration Efficiency
Gelman Spectrograde Glass Fiber	28.3	6	> 99.8%
	84.9	6	> 99.8%
Fluoropore 1 μm pore	3.0*	1	> 99.9%
	7.2, 10.8, 18.7, 27.0	1	> 99.9%
	28.3	6	> 99.9%
	84.9	6	> 99.9%
Nuclepore 0.8 μm pore	14.2	1	72%
	28.3	1	72%
	84.9	1	89%
Whatman 41, Cellulose	28.3	6	64%
	84.9	6	83%
Gelman GA-1 5 μm pore, cellulose acetate	28.3	5	> 99.1%
	84.9	5	> 99.0%
MSA 1106 BH Glass Fiber	28.3	6	> 99.2%
	84.9	6	> 99.1%
Gelman A Glass Fiber	28.3	6	> 99.9%
	70.8	6	> 99.9%
EPA Glass Fiber**	28.3	6	> 99.8%
	70.8	6	> 99.8%

*This measurement was made with the filter mounted directly on the CNC inlet.

**Recently supplied by the U.S. Environmental Protection Agency to local agencies for monitoring purposes.

make the filter structure more dense. Since the effect sets in between 28.3 and 56.6 ℓpm, it seems advisable to use sampling rates below 56.6 ℓpm when using 47 mm Fluoropore filters. Even at lower flow rates it is possible that mechanical creep might occur if the pressure drop from loading of the filter is excessive.

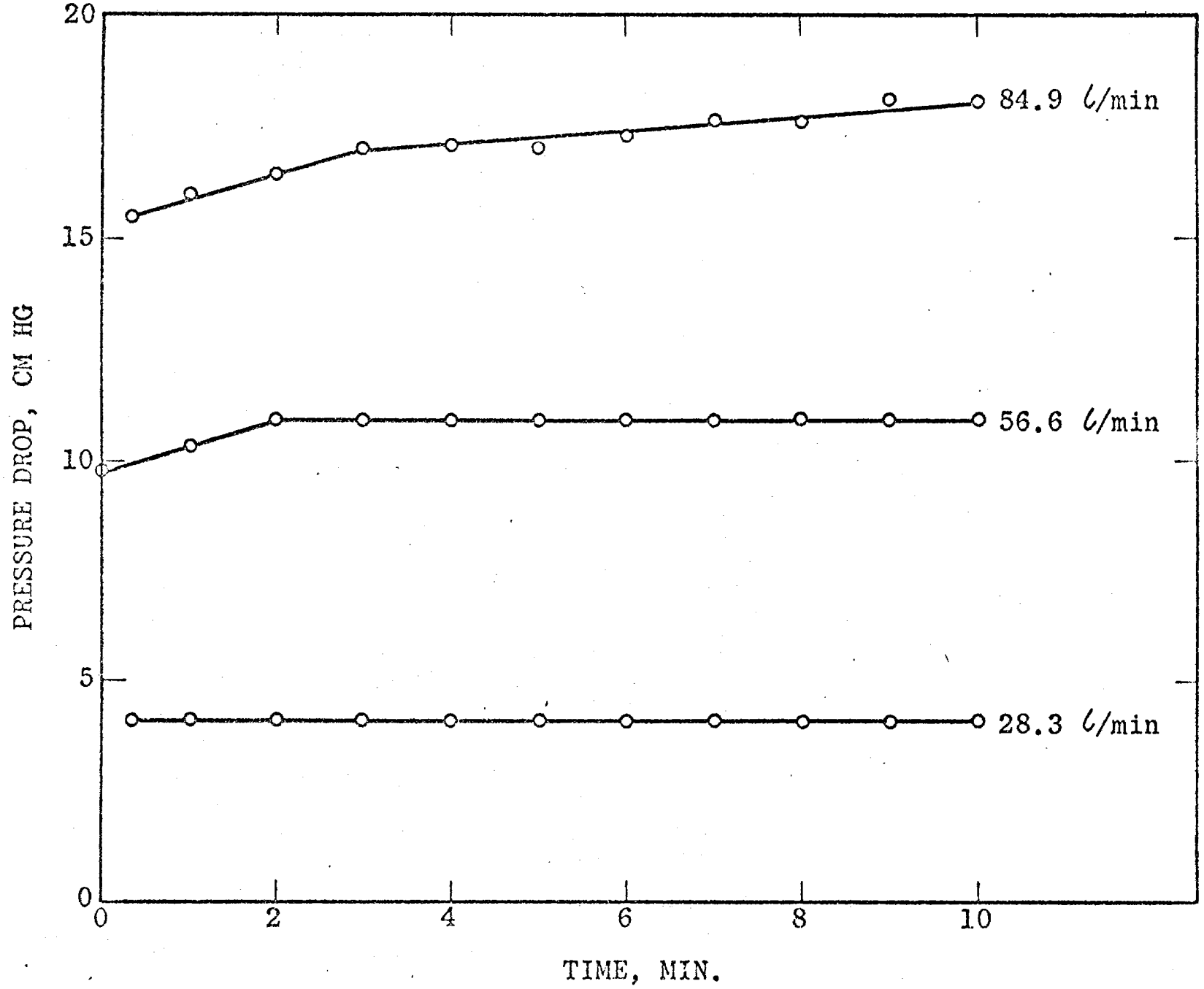

Figure 2 - Pressure drop vs. time for three different flowrates of clean air through Fluoropore filters.

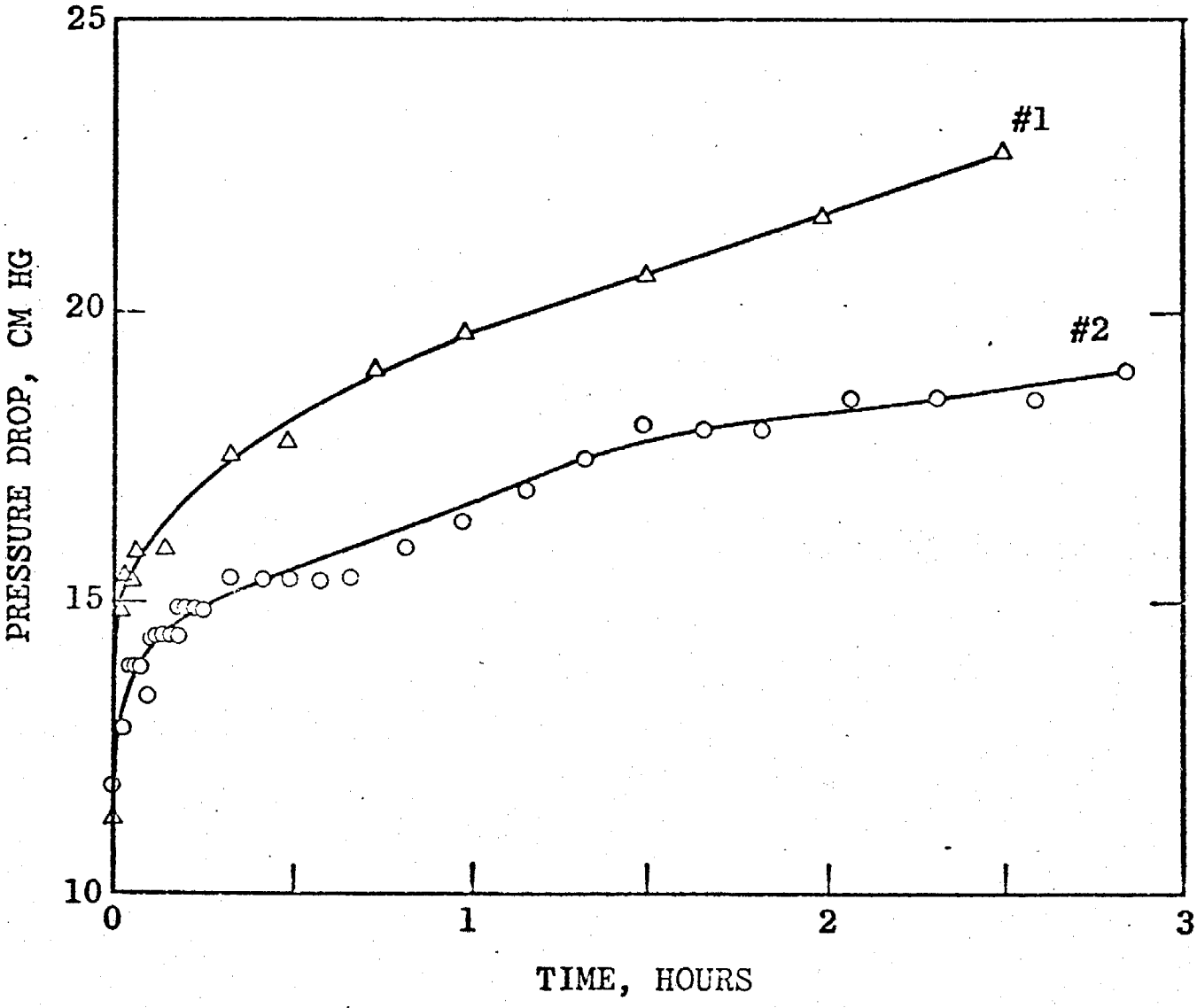

Figure 3 - Pressure drop vs. time for two examples of Fluoropore filters. Clean air flowed through the 47mm dia. filters at 84.9 l/min.

DEPENDENCE OF FILTER EFFICIENCY ON PRESSURE

It is necessary to discuss the influence of the air pressure on filtration efficiency since in the present measurements compressed air flowed through the filter whereas in sampling ambient air the flow is maintained by pumping a partial vacuum downstream of the filter. The two cases are diagrammed below where P_i refers to pressure and v_i to face velocity.

(1) Present measurements

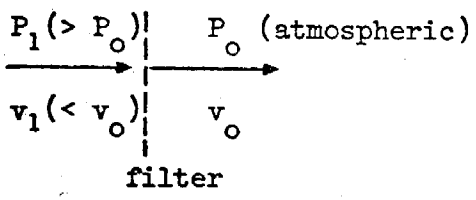

(2) Sampling ambient air

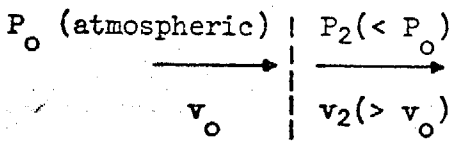

Note that the face velocity on the atmospheric pressure side of the filter is taken to be the same (v_o) in both cases since the efficiency is to be compared at the same mass flow rate. The mean pressure within the filter is greater in case (1) than in case (2) while the mean velocity is less in case (1) than in case (2).

The dependence of filtration efficiency on pressure has been studied experimentally by Stern et al.[3], who found the efficiency to increase with decreasing pressure. This implies that the present measurements give lower efficiencies than would be encountered in ambient air sampling. The Stern et al. result has been explained by Pich[4] as arising from the effect of

pressure on the slip correction. With decreasing pressure, the slip correction increases and, as a consequence, the diffusion coefficient and Stokes number increase, in turn increasing particle deposition by diffusion and impaction.

In addition to the effect from reduced pressure, the effect from residence time of the aerosol in the filter must be considered.[5] The residence time is less in case (2) than in case (1), tending to offset the increase in the diffusion coefficient. Let us take the pressure drop across the filter to be approximately 0.1 atmosphere in both case (1) and case (2). Then assuming the pressure changes are adiabatic, we find the ratio of the mean residence times in the filter to be $t_2/t_1 = 0.93$ where the subscripts refer to the case number. For 0.1 μm diameter particles, the ratio of the slip factors is $C_2/C_1 = 1.07$. For 0.01 μm diameter particles, $C_2/C_1 = 1.10$. The diffusion deposition efficiency E_D is related to the product of the diffusion coefficient and the residence time. For 0.1 μm diameter particles, $\frac{D_2t_2}{D_1t_1} = \frac{C_2t_2}{C_1t_1} = 1.0$. For 0.01 μm diameter particles, $\frac{C_2t_2}{C_1t_1} = 1.03$. Most filtration theories[6] find the filtration efficiency to depend on the product D_it_i raised to a fractional exponent such as 2/3. It can be seen, therefore, that E_{D_2}/E_{D_1} is equal to 1.0 within a few percent, a figure much less than the uncertainties of the calculation. Further, the efficiency ratio for impaction E_{I_2}/E_{I_1} will be greater than one since C_2/C_1 is greater than one, although it is not easy to estimate the magnitude from current theories.

The results obtained in the preceding discussion should be regarded as only semi-quantitative because of uncertainties and approximations in current

filtration theories. Nevertheless, the small magnitudes of the indicated corrections allow us to safely conclude that the filtration efficiencies obtained in the present measurements can be applied to the sampling of ambient air within the errors of the measurements. We further note that there are greater uncertainties associated with loading of filters in actual sampling which not only increases the pressure drop but changes other characteristics of the filter as well. The presently obtained efficiencies apply to relatively clean filters only.

ACKNOWLEDGEMENT

These measurements were made at the suggestion of B. R. Appel who contributed helpful comments. We appreciate the interest and support of J. J. Wesolowski. Glen Sasaki assisted with the laboratory measurements.

REFERENCES

1. B. R. Appel and J. J. Wesolowski, AIHL Report No. 125, March 1972.
2. B. Y. H. Liu and K. W. Lee, Envir. Sci. and Tech. 10, 345-350 (1976).
3. S. T. Stern, H. W. Zeller and A. L. Schekman, J. Colloid Sci. 15, 546 (1960).
4. J. Pich, Aerosol Science, Academic Press, N.Y., 1966, C. N. Davies, ed., pp. 248-249.
5. We are indebted to B. Y. H. Liu for pointing out the importance of residence time.
6. R. G. Dorman, Aerosol Science, Academic Press, N.Y., 1966, C. N. Davies, ed., pp. 205-210.

Appendix J

Intermethod Comparison α-XRFA Sulfur and Sulfate Values on Fluoropore Filters

Previous AIHL programs have utilized α-XRFA at Crocker Nuclear Laboratory to obtain sulfur values on atmospheric samples collected on cellulose acetate membrane filters. On average, results agreed within 10% with those obtained wet chemically although differences up to a factor of three were observed. The present comparison extended this work to include atmospheric samples collected on Fluoropore filters. The results are summarized in Table J-1 and indicate relatively poor agreement between methods. Comparing the fraction of sulfate in respirable particles as measured by the AIHL microchemical method and by α-XRFA, the latter yielded values which appear unrealistic and show high variability. By the wet chemical approach on average, about 75% of the sulfate is found in particles < 3.5 μm in both cases, a value which appears reasonable in comparison with previous data.

It is believed that Fluoropore filter samples pose unusual difficulties in correcting α-XRFA sulfur values for filter penetration effects. Studies are continuing at CNL to correct this.

Table J-1

Comparison of α-XRFA Sulfur and Sulfate Results
with Atmospheric Samples on Fluoropore Filters

Batch	α-XRFA S(as $SO_4^=$)/Sulfate	Resp/Total Sulfate[a]	
		α-XRFA	Wet Chem.
1	4.6 ± 4.4[b]	$1.04 \pm .15$[c]	$0.76 \pm .25$
2	2.0 ± 2.4[e]	1.4 ± 1.19[d]	$0.73 \pm .20$[d]

a. Ratio respirable sulfate/total sulfate obtained by the methods shown.

b. Mean of 17 values

c. Mean of 7 values

d. Mean of 8 values

e. Mean of 15 values

Appendix K

Adsorption Isotherms for SO_2-Clean Filter Interactions

The determination of adsorption isotherms for a gas while flowing through a filter can be complicated by any pressure drop across the filter and by adsorption of the pollutant on the walls of the tubing, filter holder, etc. In the present case, the flow rates were $\leq$ 1.32 cfm for 47 mm filters. Under these conditions, the pressure drop across the glass and cellulose filters was 0.5 to 0.7 psig and, for the membrane filters, 1.0 to 1.7 psig. To eliminate the anticipated error from pressure change, the downstream sample was passed through a stainless steel bellows air pump and the sample pressure to the SO_2 monitor adjusted to equal (within 0.02 inches of water) that of the upstream sample. Under these conditions, the calibration previously obtained for the Meloy unit was applicable and the downstream concentration could be directly monitored. Each isotherm was corrected for a system blank caused by adsorption on surfaces other than the filter media.

The procedure is best explained by an example. Table K-1 lists the data for an isotherm constructed for SO_2 adsorption on an MSA 1106BH glass fiber filter. The first column gives the times after initiation of sampling when the SO_2 analyzer output readings were recorded. The second column lists the downstream readings (in chart units) at the respective elapsed times, and the third shows the corresponding net chart readings obtained by subtracting the chart reading at time 0 from the values given in the second column.

A net reading of 0 indicates no SO_2 penetrating the filter. The fourth column lists the ratios, R_f, of net chart unit readings at time t to the ultimate response when the filter is observed to be completely saturated with SO_2 and penetration 100%. The ultimate response is used in place of the upstream concentration for experimental convenience, but in each case the ultimate response was shown to be equivalent to the upstream SO_2 concentration. Figure K-1 plots R_f values uncorrected for the system blank.

The data for the corresponding ratios, R_b, with no filter (system blank) are shown in Table K-2 and plotted in Figure K-2. The system blank reflects primarily the response time of the Meloy sulfur analyzer. The filter responses are corrected for the system blank by dividing each R_f by the corresponding R_b obtained at the same elapsed time (last column in Table K-1). The corrected isotherm is shown in Section V.

Table K-1

SO_2 FILTER ISOTHERM
MSA FILTER

Filter I.D.: B0405M Date: 5/27/77

RH: 50%

SO_2: 0.1 ppm

Flow: 1.32 cfm

Lag Time: 3.5 min

Elapsed Time (min)	Chart Reading	Net Reading	R_f	R_f/R_b
0	7.5	0	0	0
0.5	7.5	0	0	0
1.0	7.5	0	0	0
1.5	7.5	0	0	0
2.0	7.5	0	0	0
3	7.5	0	0	0
4.5	9.5	2	0.04	0.04
5	11	3.5	0.07	0.07
6	14.5	7	0.14	0.15
7	18	10.5	0.22	0.23
8	23	15.5	0.32	0.33
9	27	19.5	0.40	0.41
10	31.5	24	0.49	0.50
11	35	27.5	0.57	0.58
12	37	29.5	0.61	0.62
13	38	30.5	0.63	0.64
14				
15	40	32.5	0.67	0.68
16				
17	42	34.5	0.71	0.71
20	43.5	36	0.74	0.74
25	46	38.5	0.79	0.79
30	47.5	40	0.82	0.82
35	49	41.5	0.86	0.86
40	50.5	43	0.89	0.89
45	52	44.5	0.92	0.92
50	52.5	45	0.93	0.93
55	54	46.5	0.96	0.96
60	54	46.5	0.96	0.96
70	56	48.5	1.0	1.0
80	56	48.5	1.0	1.0

R_f = ratio of net SO_2 strip chart readings at time "t" to that when further change is negligible. In this case, this final net reading is 48.5.

R_b = ratio of chart reading at time "t" to that when no further change is observed when no filter is in place (a system blank).

Table K-2

FILTER ISOTHERMS
SYSTEM BLANK

Filter I.D.: None Date:

R.H.: 50%

SO_2: 0.1 ppm

Flow: 1.32 cfm

Lag Time: 0.1

Elapsed Time	Chart Reading	Net Reading	R_b
0	7.5	0	0
0.5	35	27.5	0.55
1.0	43	35.5	0.71
1.5	47.5	40.0	0.80
2.0	50	42.5	0.85
3	52.5	45	0.90
4	54	46.5	0.93
5	55	47.5	0.95
6			
7	56	48.5	0.97
8			
9			
10	56.5	49.0	0.98
11			
12			
13			
14			
15	57	49.5	0.99
16			
17			
20	57.5	50	1.0
25			
30			

Figure K-1

ABSORPTION ISOTHERM FOR MSA FILTER WITH SO_2

(Uncorrected for System Blank)

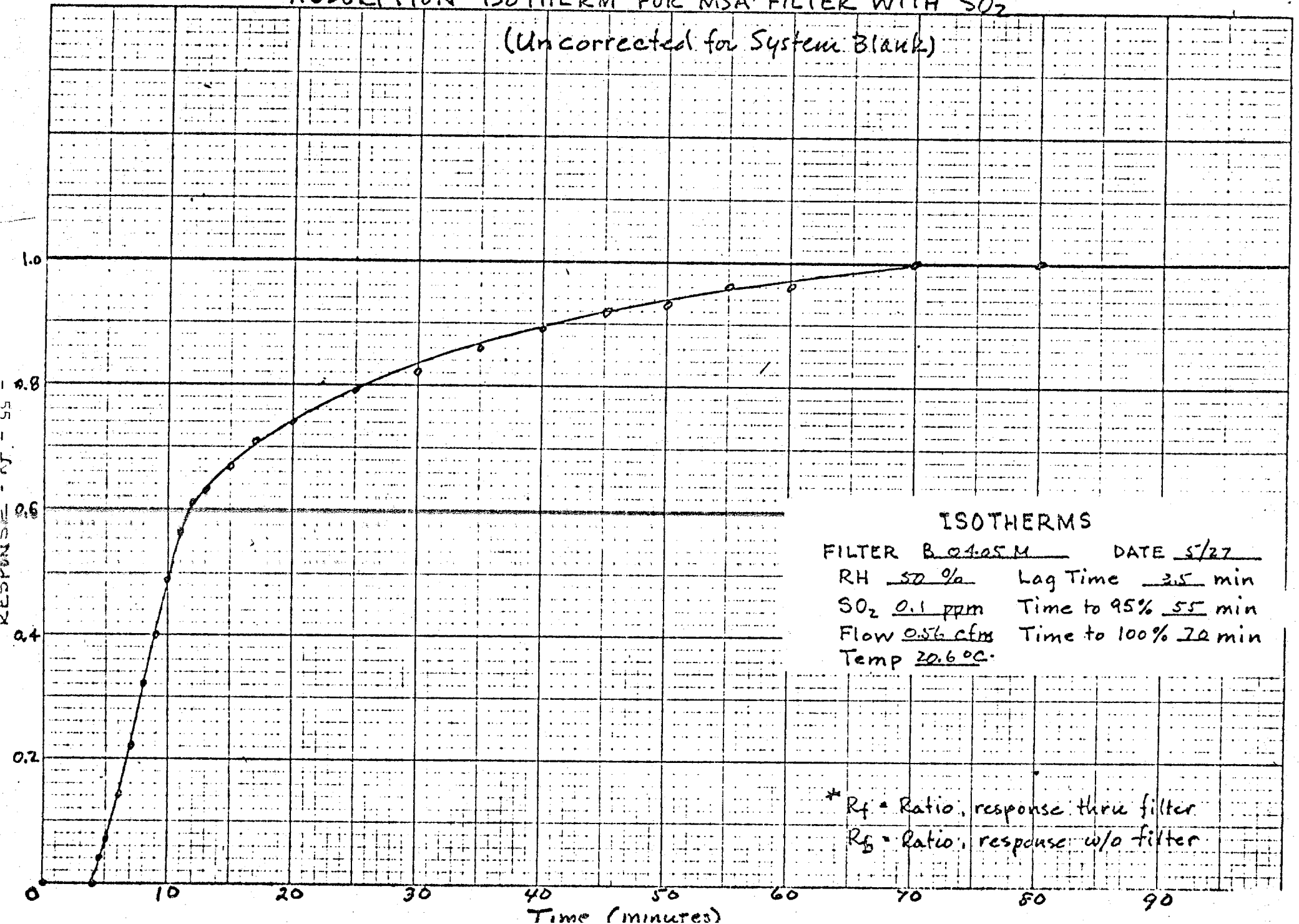

ISOTHERMS

FILTER B 01-05 M DATE 5/27

RH 50 % Lag Time 2.5 min

SO_2 0.1 ppm Time to 95% 55 min

Flow 0.56 cfm Time to 100% 70 min

Temp 20.6 °C.

* R_f = Ratio, response thru filter

R_b = Ratio, response w/o filter

Figure K-2

ABSORPTION ISOTHERM FOR EXPOSURE SYSTEM WITH SO_2

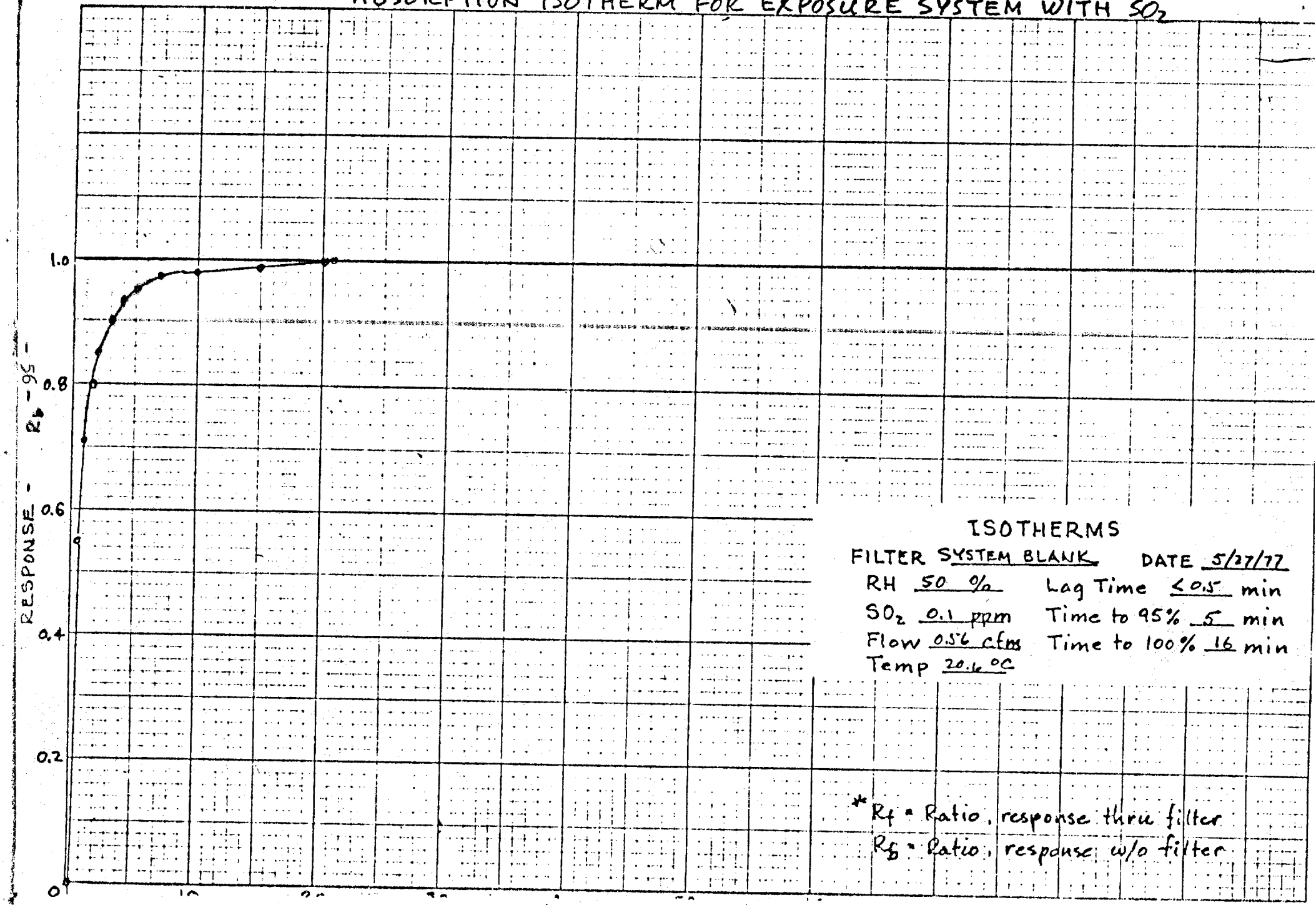

ISOTHERMS

FILTER SYSTEM BLANK DATE 5/27/77

RH 50 % Lag Time < 0.5 min

SO_2 0.1 ppm Time to 95% 5 min

Flow 0.56 cfm Time to 100% 16 min

Temp 20.6 °C

* R_f = Ratio, response thru filter
R_b = Ratio, response w/o filter

Appendix L

Nitrate Contamination of the Exposure System

Following trials with NO_2-O_3 mixtures, subsequent filter exposures with NO_2 alone exhibited greatly enhanced artifact nitrate levels. The degree of this enhancement appeared to diminish with time. Figure L-1 illustrates the extent of this error as a function of time following the NO_2-O_3 runs. Throughout this period, the system was being continually purged with purified air. The results shown represent only the apparent error due to system contamination; each result was corrected for the extent of artifact nitrate contributed by NO_2-filter interactions as measured in a clean system. The observed system error can be substantial, representing 2 or 3 times the level due to clean filter interaction with NO_2. Retention and desorption of HNO_3 from the walls followed by collection of the acid on filters is the likely cause of the system error.

Enhanced nitrate levels on filters were also observed in NO_2 exposures which followed a series of runs employing only SO_2 under varying conditions. The latter runs were made following cleaning of the inner walls. It appears that contamination of walls by sulfuric acid leads to NO_2 to nitrate conversion on the walls followed by desorption and filter collection as nitric acid. Further work is necessary to confirm this.

Cleaning of the system was done by immersion and scrubbing with detergent and water followed by a distilled water rinse and air drying.

The effect of nitrate contamination on the results included in this report is probably minor; in those cases where contamination was evident, results are expressed only as a change in observed nitrate produced by the addition of the test variable.

Figure L-1

NITRATE COLLECTION ON FILTERS DUE TO EXPOSURE SYSTEM CONTAMINATION

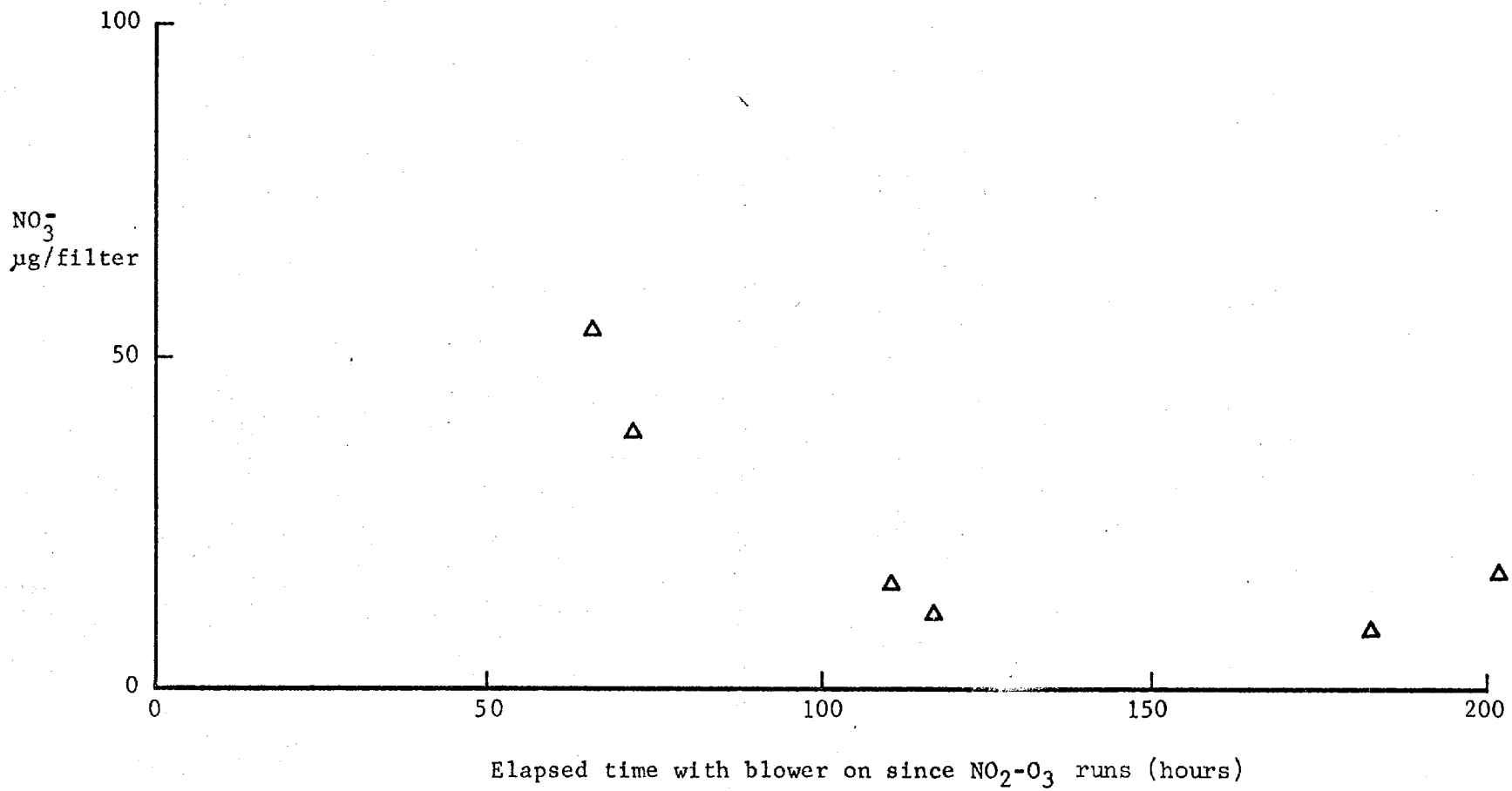

Appendix M

Preparation of Filters Loaded with Potential Catalysts for SO_2 Oxidation

Introduction

The conversion of SO_2 to artifact sulfate may be catalyzed by certain constituents in ambient aerosols. To load filters with particles for subsequent exposure to SO_2, monodisperse aerosols of $Fe(OH)_3$, V_2O_5, $Cu(OH)_2$ and MnO_2 were generated and collected on 47 mm MSA and Fluoropore filters. The target particle size was 1-2 μm (optical diameter) which represented a compromise between expected ambient particle sizes (i.e., sub-micron in aerodynamic diameter) and limitations in equipment and time. The target loadings were based on maximum observed atmospheric values reported for two-hour samples in the ACHEX. For Mn, Cu and V, these were increased by a factor of 5 to 10 to allow for the possible enrichment in sampling the Los Alamitos power plant plume, or enhanced levels from wind-blown dust.

Experiment Description

The monodisperse aerosol was generated from a Model 50A Berglund-Liu vibrating orifice generator passed through a K^{85} charge neutralyzer and dispersed into a plexiglas plenum (Figure M-1). The Berglund-Liu dilution and dispersion air flow rates were $6M^3$/hr and 15 cc/min, respectively, throughout the experiment. A Deltech double column compressed air dryer was used to supply low humidity air to the system. The air was heated slightly above room temperature before entering the system.

The aerosol size was monitored by a Climet OPC (optical particle analyzer). Readout systems included a Tracor-Northern MCA (multi-channel analyzer) for size distribution display and an Ortec line printer for total particle count. A chart recorder and oscilloscope were used for constant aerosol concentration monitoring and pulse height display, respectively.

The manifold was constructed to load filters simultaneously with aerosol from the plenum. Three Nuclepore filter holders were placed symetrically at the base of the cylindrical manifold to achieve equal loading, assuming an equivalent volume of air passed through each. To ensure equivalent sampling volumes, two Sierra dual flow controllers were used to draw the air through the filters. The air flow rate was maintained at approximately 27 ℓ/min and checked prior to each run with a Gilmont rotometer. To prevent conglomerated particles from falling onto the filters two 90-degree bends were employed between the plenum and manifold. Plenum overflow was exhausted at atmospheric pressure into a hood for operator safety.

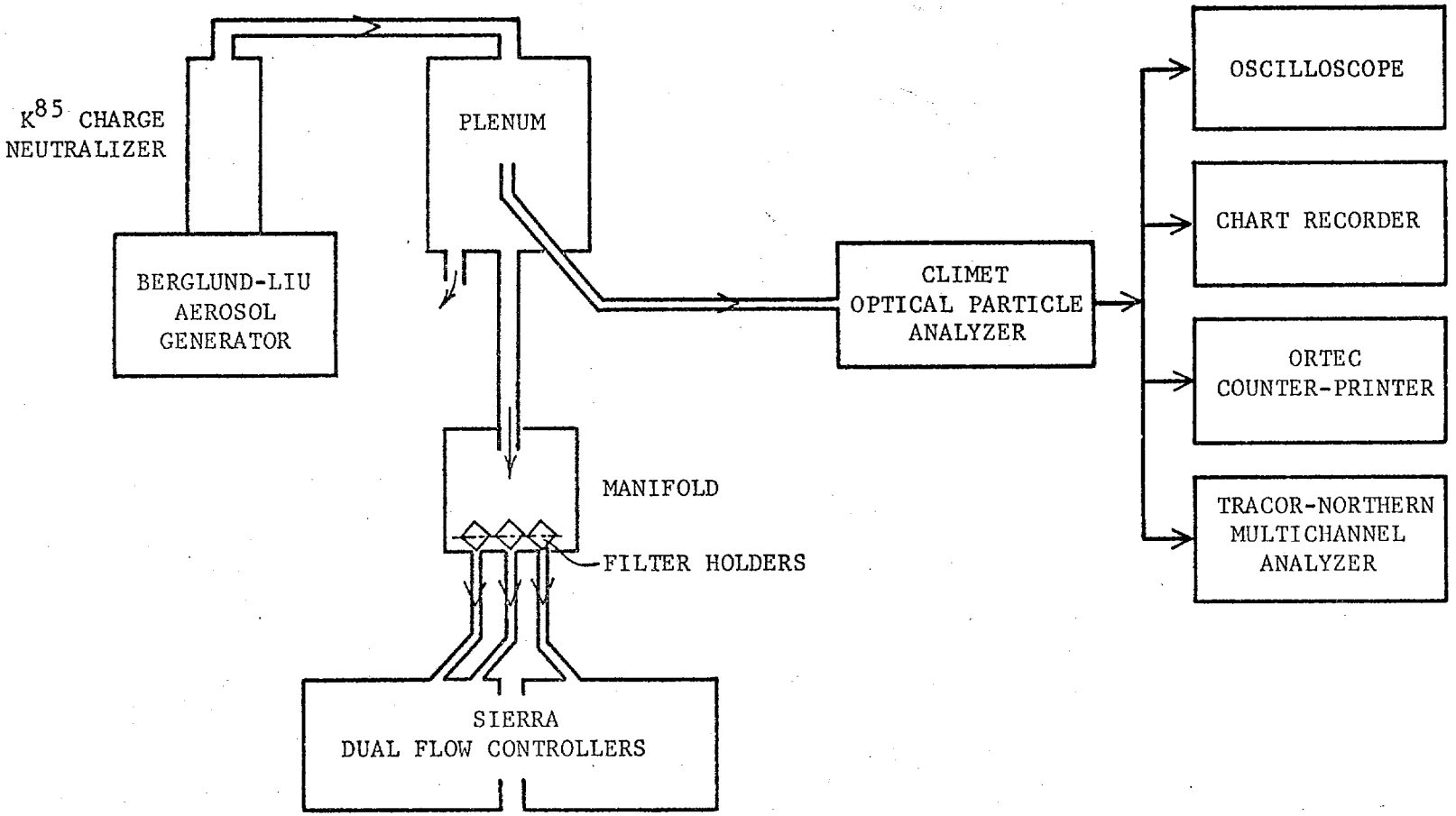

SYSTEM FOR LOADING OF FILTERS WITH POTENTIAL OXIDATION CATALYSTS

Figure M-1

To check the precision between filters of the aerosol deposition, six Millipore (AAWP) cellulose acetate 47 mm membrane filters were loaded (in two runs) with 240 and 77 µg of 1.5 µm methylene blue (Mb) aerosol to simulate catalyst loading, and analyzed by spectrophotometry. Loading differences among the three filters in the first and second runs were ± 1% and ± 2% of the totals, respectively. In addition to methylene blue, the precision for loading three filters simultaneously with each metal oxide was also determined (Table M-1). The results indicate, in general, a coefficient of variation of < 10%.

Chemical and Physical Properties of the Aerosols

Table M-2 describes the chemistry involved in the loading of the filters. In each case, in addition to the suspected catalyzing compound loaded onto the filters, there are also by-products. In the cases of vanadium, iron and copper oxides/hydroxide aerosols, ammonium nitrate is a constituent of each particle. However, upon impaction on the filter and exposure to humid air, the ammonium nitrate deliquesces, leaving the metal oxide/hydroxide exposed, as observed with MSA glass fiber filters or in a pool of hydrated NH_4NO_3 as observed for the hydrophobic Fluoropore filters.

A great deal of work was done to develop a technique to obtain MnO_2 aerosol. A colloidal suspension of MnO_2 proved unsuccessful since it coagulated in the Berglund-Liu, clogging the prefilters and orifice. To overcome this problem, pure $KMnO_4$ aerosol was generated, loaded on filters and later reduced to MnO_2 plus Mn_2O_3 by exposure to formaldehyde vapor. This approach had the disadvantages of the uncertainty in chemical state of the manganese and the likely formation of a basic salt, potassium formate, as a co-product.

Table M-3 shows the physical properties of the aerosol generated for this study. The cause of the deviations of calculated from the microscopy sizing are unclear. Copper hydroxide was difficult to observe by microscopy and no good estimate of size could be given. The manganese dioxide samples were unavailable for sizing after the formaldehyde conversion. The calculated sizes shown on Table M-3 based on a comparison of loading density with MnO_2 samples are those of the metal oxide/hydroxide only and neglects the ammonium nitrate, if present. The intended loading of metal ion catalyst per filter varied from 150 µg to 50 µg.

Table M-1

Precision for Loading Filters from Three Filter Manifold

Catalyst	Filter	C.V. (%)	
		Basis 2 Filters	Basis 3 Filters
$Fe(OH)_3$[a]	Fluoropore	5.2	---
	MSA 1106BH	6.6	
V_2O_5	Fluoropore	6.1	---
	MSA 1106BH	10.7	22.6
$Cu(OH)_2$[a]	Fluoropore	5.7	---
	MSA 1106BH	3.7	---
MnO_2[b]	Fluoropore	13.2	---
	MSA 1106BH	2.7	3.7

a. Probably exists as a mixture of the oxide and hydroxide.

b. Probably exists as a mixture of MnO_2 and Mn_2O_3.

Table M-2

Chemical Reactions

Aerosol Solution (Expressed as Molar Concentrations)	Products Loaded on Filter	Remarks
I. $[8.3 \times 10^{-4}]$ $Fe(NO_3)_3$ $[3.4 \times 10^{-4}]$ NH_4OAC	$Fe(OH)_3$ NH_4NO_3	Excess NH_4OAC volatilizes
II. $[4 \times 10^{-4}]$ NH_4VO_3 $[4 \times 10^{-4}]$ HNO_3	V_2O_5 HN_4NO_3	
III. $[5.5 \times 10^{-4}]$ $CuNO_3$ +25 ml saturated NH_3/liter	$Cu(OH)_2$ NH_4NO_3	Excess NH_3 volatilizes
IV. $[4.5 \times 10^{-3}]$ $KMnO_4$	$KMnO_4$ ↓ Formaldehyde Treatment MnO_2 + by-products (potassium formate?)	Formaldehyde treatment after loading

Table M-3

Physical Properties of Metal Aerosols

Catalyst	Calculated Size	Size by Microscopy	Metal Loading Target	
			$\mu g/m^3$	$\mu g/47$ mm Filter[a]
$Fe(OH)_3$	1 μm	1.5 μm	5[b]	150
V_2O_5	1 μm	2 μm	1[c]	50
$Cu(OH)_2$	1.5 μm	---[e]	1[d]	50
MnO_2	2.2 μm	f	1[d]	50

a. Calculated to relate to sampling of 1500 m^3 of air at the metal concentration shown.

b. Maximum observed in ACHEX.

c. A factor of 5 higher than observed in ACHEX allowing for sampling of power plant plume.

d. A factor of 10 higher than observed in ACHEX, assumed to represent an upper limit to values expected in ambient air.

e. Not readily visible by microscopy.

f. Not available for sizing following formaldehyde reduction.

Appendix N

Carbon as a Catalyst for SO_2 to Sulfate Conversion

Three experiments were conducted in cooperation with Dr. T. Novakov and co-workers at the Lawrence Berkeley Laboratory to evaluate the effects of combustion derived carbon ("soot") in converting SO_2 to sulfate.* The sulfate observed in these experiments represents not only sulfate and/or sulfite associated with carbon-SO_2 interactions (both suspended carbon and carbon on filters) but also sulfate from SO_2-filter media interactions, and SO_3 and sulfate formed in the flame from sulfur compounds in the acetylene used as the fuel. The system for generation and collection of carbon plus sulfate is shown in Figure N-1. The experiments were as follows:

1. SO_2 was injected downstream of an acetylene flame in a region with temperature about 300°C. Filter collection of the aerosol was made using 47 mm Gelman glass fiber filters at 1.32 cfm. Two filters sampled for 10 hours continuously while, on the remaining two holders, filters were changed after five hours.

2. As in 1, but no SO_2 injected. This experiment was made to evaluate the significance of sulfate formed from sulfur compounds in the acetylene fuel. In addition, the volatility behavior of the soot collected on the filters was evaluated to obtain the proportion of relatively volatile, organic carbon.

3. No SO_2 injected. Two sets of four filter samples were (on Gelman A) collected, sampling for five hours with each set. The filters were subsequently exposed to SO_2 under varying humidity conditions using the AIHL exposure system.

Experiment 1 was designed to provide an upper limit to the level of sulfate expected in ambient air as the result of carbon catalysis from suspended particles, since the temperature of the carbon-added SO_2 mix was initially high. The results are summarized in Table N-1 and indicate a sampling precision of 11% (C.V.) or better for carbon. The sulfate levels, with one exception, were significantly greater than those expected from SO_2-clean filter interactions alone. It was previously established that clean Gelman A exposed to 0.1-0.5 ppm SO_2 is saturated with SO_2 in 10 minutes at the flow rate used here (1.32 cfm). If most of the observed sulfate resulted from SO_2 - filter interactions then the ratio sulfate/carbon should decrease with increasing sampling time. The observed ratio

*Under wet chemical analysis conditions, the sulfate observed represents sum of sulfate plus sulfite.

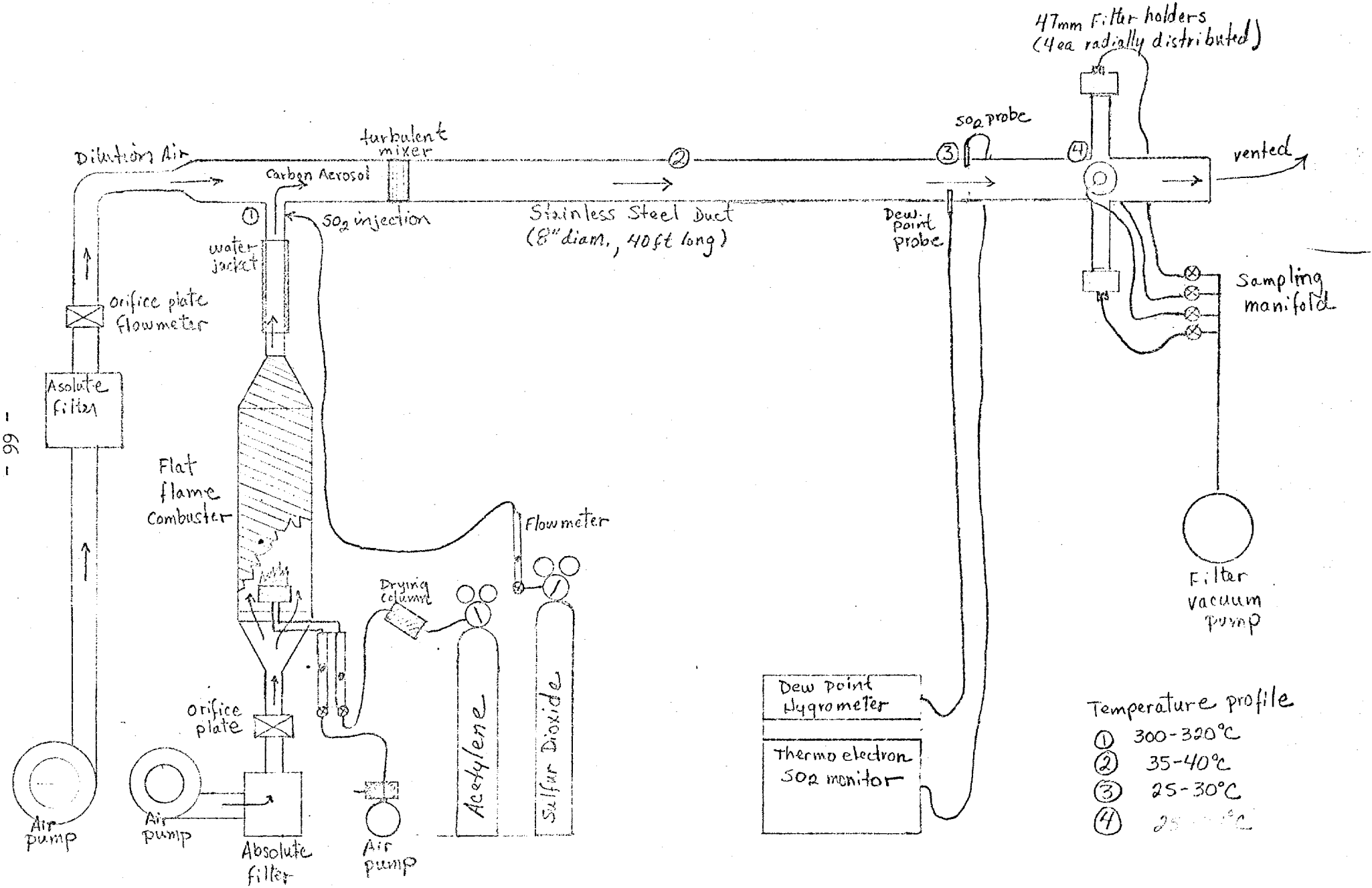

Figure N-1. SO_2 - Particulate Carbon Exposure System

Table N-1

Results of Simultaneous Collection of Combustion Derived Soot and Sulfate on Gelman A Filters with Added SO_2 (Experiment 1)[a]

Filter I.D.	Sampling Time (hrs)	Average SO_2 (ppm)	Carbon Collected (μg)	Sulfate Collected (μg)	Expected Sulfate (μg)[c]	Sulfate as % of Carbon	% SO_2 Converted to Sulfate[d]
B 0041A	1st 5	0.18	457.7				
				70.3[b]	48	9	0.32
B 0045A	2nd 5	0.34	307.1				
B 0042A	1st 5	0.18	534.1	82.0	44	15	1.03
B 0046A	2nd 5	0.34	321.2	17.2	51	5	0.12
B 0043A	10	0.26	828.3	107.5	48	13	0.49
B 0044A	10	0.26	750.7	83.0	48	11	0.37

a. Exposure conditions: Average Relative Humidity at filters = 32%
Temperature at filters = 24.6 ± .9°C
Temperature at SO_2 injection point = 297 ± 6°C

b. Filters 41A and 45A combined and extracted together. The amount shown is the total sulfate for the two 5-hour filters.

c. Resulting from SO_2-filter interactions and calculated from adsorption isotherm data at 50-60% R.H., interpolating between results with 0.1 and 0.5 ppm SO_2.

d. % SO_2 converted $= \dfrac{(\mu g\ SO_4^{=}\ \text{observed})\frac{64}{96}}{(\text{ppm } SO_2)\ (2620)(m^3)} \times 100$

was not significantly different for samples collected for five and ten hours. Accordingly much of the sulfate and/or sulfite appears to relate either to fuel sulfur oxidized in the flame or to carbon-SO_2 interaction.

The sulfate levels in Experiment 1 represented 5-15% of the weight of carbon collected and 0.1-1.0% of the SO_2 passing through the filter. If carbon collected on a filter was able to convert SO_2 to sulfate (or fix SO_2 as sulfite) without being saturated then the sulfate observed on 10-hour filter samples would exceed the sum of the sulfate observed on the two successive five-hour samples. The observed mean sum, for two trials, 85 $\pm$ 20 µg compares to the mean 10-hour value 95 $\pm$ µg. Thus, if carbon was functioning as a catalyst, it was relatively ineffective.

The SO_2 concentration measured near the filters varied from 0.18 to 0.34 ppm as five-hour average values. At the conclusion of the experiment the flame was turned off and the instantaneous SO_2 concentrations was observed to decrease from 0.41 to 0.13 ppm. This implied that the difference, 0.28 ppm SO_2, resulted from oxidation of the sulfur compounds present in the acetylene. The ratio of fuel-related/added SO_2 was, at that moment, 2.2. This ratio at other times during the experiment is unknown.

The LBL staff tried various techniques to obtain sulfur-free acetylene but was unsuccessful. Accordingly, the second experiment was run to serve as a "blank" for Experiment 1; no SO_2 was added to the system. The results are shown in Table N-2 and indicate a reduced level of sulfate collected, in µg, but a similar level of sulfate, expressed as a percent of carbon, to that in the first experiment. Thus, it appears that most, if not all, of the observed sulfate in Experiment 1 was due to fuel sulfur which had been oxidized to SO_2, SO_3, and/or sulfate by the flame and that SO_2 added downstream of flame remained almost completely unconverted even though the temperature was initially high. In two cases, the sulfate observed was less than that expected from SO_2-filter interactions. The cause of this behavior is unclear.

As part of Experiment 2 the volatility behavior of the collected soot was studied. It was hoped to provide some insight into the level of soot-related organic carbon from the acetylene flame. For this purpose, a series of one cm^2 discs were cut from a 10-hour loaded Gelman A filter. Two discs were analyzed without heating and the remaining three heated in a stream of air as follows:

a. All for 1 hour at 100°C.

b. Following a., two for 1 hour at 150°C.

c. One of the two from b. heated for one hour at 200°C.

The results are shown graphically in Figure N-2 and indicate about 40-45% loss $\geq$ 150°C. The plateau in the graph suggests little further loss would be expected up to pyrolysis and/or combustion temperatures. The carbon remaining non-volatile at $\leq$ 200°C, can be used here as an upper limit estimate of the graphitic carbon present in the soot.

Table N-2

Sulfate Observed from an Acetylene Flame Without Added SO_2 (Experiment 2)[a]

Filter I.D.	Sampling Time (hrs)	Average SO_2 (ppm)	Carbon Collected (µg)	Sulfate Collected (µg)	Expected Sulfate (µg)[b]	Sulfate as % of Carbon	% SO_2 Converted to Sulfate[c]
B 0047A	1st 5	.16	412.4	56.8	43	14	0.81
B 0051A	2nd 5	.14	383.8	28.8	42	8	0.47
B 0048A	1st 5	.16	427.6	64.8	43	15	0.91
B 0052A	2nd 5	.14	369.5	26.7	42	7	0.44
B 0049A	10	.15	693.6	89.4	43	13	0.69
B 0050A[d]	10	.15	705.4	65.4	43	9	0.51

a. Exposure conditions: Average Relative Humidity at filters = 41%
Temperature at filters = 28 ± 2

b. See footnote c, Table 1.

c. See footnote d, Table 1.

d. Used in control experiment to evaluate volatile C.

Figure N-2

LOSS OF ACETYLENE-DERIVED PARTICULATE CARBON WITH TEMPERATURE

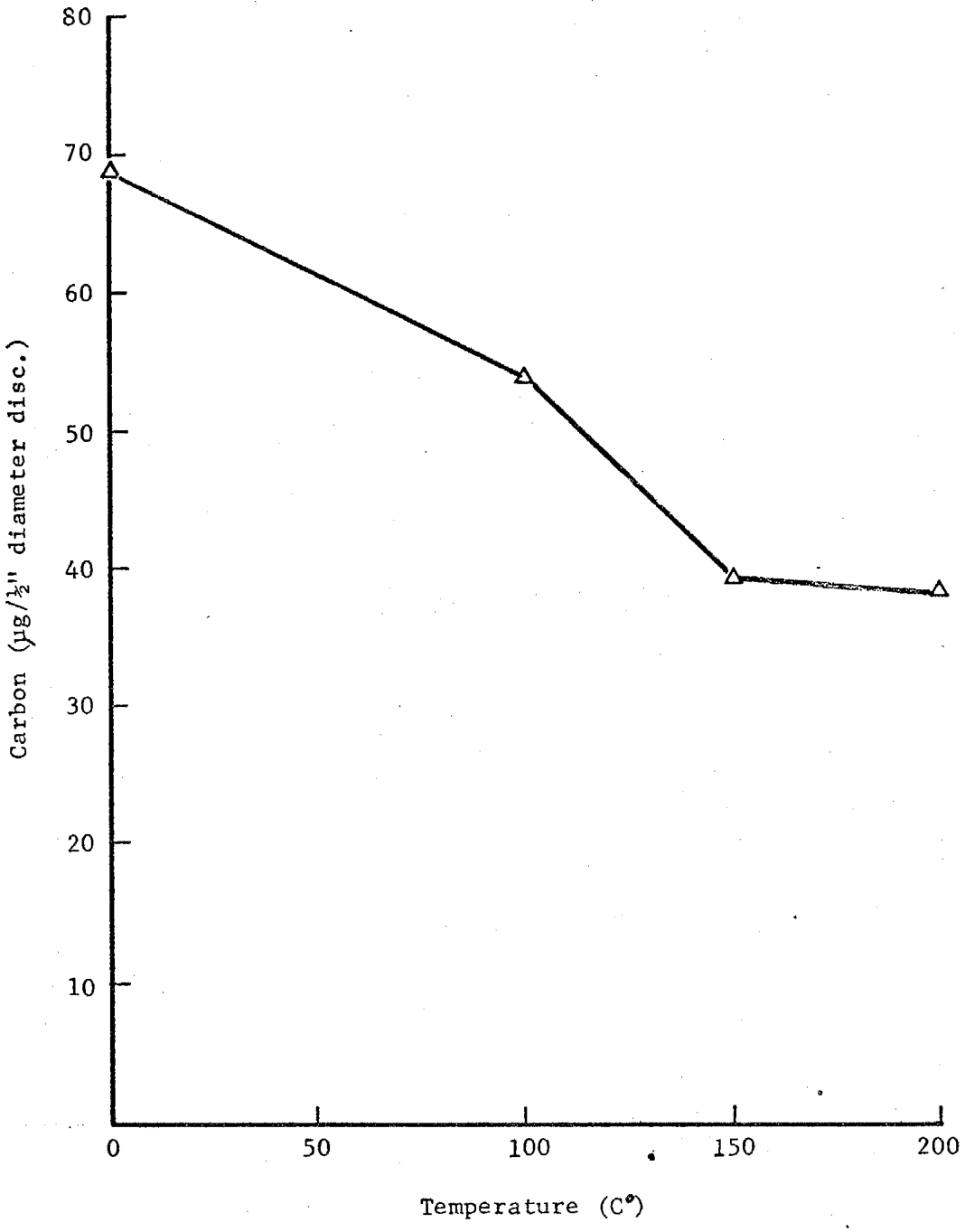

In the third experiment the carbon-loaded filters were subsequently exposed to 0.1 ppm SO_2 at two relative humidities, 50 and 90%. Because of the fuel sulfur, filters contained an initial sulfate level prior to deliberate SO_2 exposure. The results are shown in Table N-3. Interpretation of these results is complicated by several factors. Carbon was collected on the filters in two batches of four each. Within each batch the carbon level collected varied from filter to filter (mean C.V. - 25%). Since the filters were collecting fuel-related sulfate as well, the µg sulfate would be expected to show similar variation.

In Experiments 1 and 2 the sulfate observed ranged from 5 to 15% of the carbon formed. The sulfate observed in Experiment 3 remains in all cases, within this range following SO_2 exposures. In the series run at 50% R.H. the sulfate, as a percent of carbon, appears to decrease with increasing exposure to SO_2 while at 90% R.H., an increase was noted. However, the expected variability in the control samples (7-15%) with zero SO_2 exposure, prevents conclusions of significant sulfate formation at 90% R.H.

We conclude that conversion of SO_2 to sulfate on soot does not appear to be a significant phenomenon either on suspended soot particles or on soot pre-collected on filters under the conditions studied here. Additional runs similar to Experiment 1, but with higher added SO_2 concentrations would be desirable. Use of alternate fuels (e.g., propane) may eliminate the complications posed by fuel-related sulfur.

Table N-3

Sulfate Observed with SO_2 Exposure on Filters Pre-Loaded with Soot (Experiment 3)

0.1 ppm SO_2 50% R.H.

Filter I.D.	Sampling Time (Hours)[a]	Carbon (µg)[b]	Sulfate Collected (µg)	Sulfate as % of Carbon
B 0053A	0	391.7	52.5	13
B 0054A	6	442.9	50.3	11
B 0055A	6	449.2	47.9	11
B 0056A	24	633.7	51.4	8

0.1 ppm SO_2 90% R.H.

B 0057A	0	299.4	21.4	7
B 0058A	6	353.6	23.8	7
B 0059A	24	527.2	44.3	8
B 0060A	24	517.5	55.6	11

a. Exposure time to 0.1 ppm SO_2 not including the time for pre-loading the filters.

b. Conditions during the initial exposure for loading filters with carbon:

SO_2 concentration (from fuel) = .19 $\pm$ .01 ppm

Relative Humidity at filters = 71 $\pm$ 3%

Temperature at filters = 29 $\pm$ 2°C

Appendix O

ARTIFACT SULFATE FORMATION DUE TO INCREASED ALKALINITY IN FILTERS LOADED WITH MANGANESE OXIDE

The presence of manganese oxides (MnO_2 and/or Mn_2O_3) formed by the formaldehyde reduction of potassium permangate was shown to enhance substantially the collection of SO_2 (measured as sulfate) on MSA 1106BH and Fluoropore filters. However, since the formation of alkaline co-products (e.g., potassium formate) was considered possible, conclusions regarding the ability of manganese oxides in the +3 and/or +4 oxidation states to enhance sulfate formation were considered equivocal.

In an effort to resolve this issue, filter media were spotted with aqueous solutions of potassium permanganate, the water evaporated, the resulting solid reduced with formaldehyde, and any changes in alkalinity monitored by pH determination. Because Fluoropore filters are not wet by aqueous solutions, Gelman A filters (pH = 7.6) were used in place of Fluoropore.

pH measurements were made following immersion in 20 ml of distilled water and 10 minutes stirring. This differs from the EPA procedure used in characterizing filter media in not employing neutral KCl solution. This was done for convenience since only changes in pH were needed for samples of approximately constant ionic strength.

The results (Table O-1) indicate an increase from 0.1 to 0.2 pH units following formaldehyde treatment. Using 0.2 as upper limit to the pH change, the maximum SO_2 fixation ascribable to direct neutralization by the corresponding increase in alkalinity (as OH^-) can be calculated. The pH change corresponds to an increase of 3.48×10^{-4} moles/20 ml solution in hydroxide ion concentration. Assuming equivalence between this increase and expected increase in moles of sulfate due to increased alkalinity, 33 µg sulfate can be determined as an upper limit to the expected increase in sulfate per filter.

Table O-1

Changes in Alkalinity of Filter Media During Preparation of Manganese Oxides (pH values)[a,b]

Filter Type	Without HCHO Treatment	With HCHO Treatment[d]	ΔpH
MSA + 100 μg $KMnO_4$[c] (as Mn)	9.50 ± .04	9.69 ± .02	+0.19
Gelman A + 100 μg $KMnO_4$ (as Mn)	8.06 ± .01	8.17	+ .11

a. All pH determinations were made within a period of 2 hours minimizing effect of instrument drift.

b. Where errors are shown, values are mean values ± 1σ for two trials.

c. After spotting of filters, solutions air-dried in particle free air overnight.

d. Exposed to vapors of liquid formaldehyde in closed container for 2 hours.